JAERI-M
5867

EXPERIMENT AND ANALYSIS OF B_4C SIMULATING CONTROL ROD ON FCA V-3 ASSEMBLY(I)

— Neutron Source Multiplication Method —

November 1974

N. MIZOO, Y. MATSUNO*, H. MAEKAWA
T. IIJIMA, K. KOBAYASHI**, T. NAKAMURA
and J. HIROTA

日本原子力研究所
Japan Atomic Energy Research Institute

JAERI-M 5867

Experiment and Analysis of B_4C Simulating Control Rod on FCA V-3 Assembly (I)

Neutron Source Multiplication Method

Nobutatsu MIZOO, Yoshiaki MATSUNO*, Hiroshi MAEKAWA,
Tsutomu IIJIMA, Keiji KOBAYASHI**, Tomoo NAKAMURA
and Jitsuya HIROTA

Division of Reactor Engineering, Tokai, JAERI

(Received March 1972)

Reactivity worths of the B_4C simulating control rods have been measured and analysed on FCA V-3 Assembly which was constructed as the engineering mock-up for Experimental Fast Reactor "JOYO". Assembly V-3 differs from JOYO in the blanket composition and the simulating control rod is 1/2 of that of JOYO in size. We have made efforts to check the adequacy of the nuclear design method and to improve the design accuracy for JOYO by determining the range of ratios of the theoretical to experimental values (C/E).

The reactivity worth of the B_4C control rod is obtained by the measurement of the sub-criticality of the system containing the control rod. In the present work the neutron source multiplication method was employed. In the calculation we employed the multigroup diffusion approximation for the core and blanket, and the collision probability method for the effective cross sections of the B_4C simulating control rod region. The cross section set used in the calculation is JAERI FAST Version 2.

The lowest limit of the sub-criticality of the system is -6 % $\delta k/k$ and the C/E ranges from 1.00 to 1.03 in the present work.

Work performed under contracts between Power Reactor and Nuclear Fuel Development Corporation and Japan Atomic Energy Research Institute (JAERI).

* Department of Nuclear Power, Toshiba Electric Co., Ltd.
** Research Reactor Institute of Kyoto University.

FCA V－3集合体におけるB_4C模擬制御棒実験と解析(I)
中性子源増倍法

東海研究所原子炉工学部高速炉物理研究室
溝尾 宣辰・松野 義明*・前川 洋
飯島 勉・小林 圭二**・中村 知夫
弘田 実弥

（１９７２年３月受理）

高速実験炉「常陽」の Engineering mockupを目的として構成されたFCA V－3集合体において，B_4C模擬制御棒の反応度価値の測定と解析を行った。V－3集合体は「常陽」とブランケット組成に大きな差異がある上，実験に使用するB_4C模擬制御棒も常陽のそれの $1/2$ サイズである。したがって，われわれは計算値対実験値の比（C／E）の存在する範囲を追求することにより，「常陽」の設計計算方式の妥当性を検定し，設計精度の向上に資することとした。

模擬制御棒の反応度価値を測定することは，体系の未臨界度を測定することに帰し，本稿では中性子源増倍法による実験値を示す。計算はすべてJAERI－FAST version 2を用いて行い，炉心およびブランケットについては均質拡散近似を使用し，B_4C模擬制御棒領域の実効断面積の計算には衝突確率法を使用した。

本研究で取扱った未臨界度の下限は－6％δk／k に及ぶが，この範囲で C／E は概ね 1.00～1.03 に収っていることが判明した。

本報告書は日本原子力研究所が動力炉核燃料開発事業団の委託によって行った研究の成果である。

＊東京芝浦電気㈱原子力本部　　＊＊京大原子炉実験所

Contents

Page

1. Preface 1

2. Critical experiments on FCA V-3 assembly 7
   2.1 An outline of V-3 assembly 7
   2.2 Critical approach 7
   2.3 Calibration of control rod 9
   2.4 Critical mass of V-3 clean system 10

3. Experimental values of B_4C simulating control rods obtained by the neutron source multiplication method 14
   3.1 Experimental procedure 14
      3.1.1 Outline 14
      3.1.2 Fundamental principle of experiment .. 15
      3.1.3 Experimental method 16
      3.1.4 Measuring system 20
      3.1.5 Averaging of measured values 22
   3.2 B_4C simulating control rod 22
      3.2.1 Simulating control rod 22
      3.2.2 Comparison with JOYO control rod 23
   3.3 Experimental results 26
      3.3.1 Experimental values 26
      3.3.2 Experimental accuracy 30
      3.3.3 Interaction effect 31
      3.3.4 Discussion on experiments 32

4. Calculated values of the reactivity worth of B_4C simulating control rod 34
   4.1 Calculation procedure 34
      4.1.1 Outline 34
      4.1.2 Collapsing of group constants 34
      4.1.3 Buffer region 36
      4.1.4 Fission spectrum 37
      4.1.5 Effective cross section of B_4C 7-pin cluster 37
      4.1.6 Effect of space meshes 42
      4.1.7 Calculation of transverse buckling ... 42
      4.1.8 Two-dimensional X-Y calculation 44
   4.2 Criticality 48

4.2.1 Outline 48
4.2.2 Comparison with experiments 48
4.3 Calculation of kinetic parameters 50
4.4 The results of calculation of reactivity worth 52
4.4.1 Definition of reactivity worth 52
4.4.2 Calculated values of reactivity worth . 52
4.4.3 Calculated values of interaction effect 52

5. A study of the ratio of calculated to experimental values 55
5.1 Outline 55
5.2 Primary comparison (C/E raw data) 55
5.2.1 Comparison of B_4C simulating control rod reactivity worths 55
5.2.2 Comparison of interaction factors 58
5.3 Correction of raw data 58
5.3.1 Correction of experimental values 58
5.3.2 Correction of calculated values 60
5.4 Secondary comparison (C/E corrected) 63

6. Conclusion and problems to be solved in the future 66
6.1 Conclusion 66
6.2 Problems to be solved in the future 67

Acknowledgement 67

Bibliography 69

Appendixes 70
Appendix (A1) Drawer loading patterns 70
Appendix (A2) Position dependence of the subcriticality to be observed ... 70
Appendix (A3) Comparison of averaging operations 70
Appendix (A4) Survey of collapsing effect ... 71
Appendix (A5) Other surveys 77
Appendix (A6) Calculation of B_4^2 80
Appendix (A7) Comparison of kinetic parameters between 8-group two-dimensional calculation and 25-group one-dimensional calculation 81
Appendix (A8) Stroke curve 83
Appendix (A9) Chemical analysis of B_4C (Denka) and isotopic ratio (PNC) 83

1. Preface

The V core of the FCA assembly has been designed for the mock-up experiment for the Experimental Fast Reactor "JOYO" and the physics mock-ups were constructed on V-1 and V-2 assemblies.[1),2)] The V-3 assembly was built as the engineering mock-up, designed to simulate the outside diameter of the core and other dimensions of "JOYO". The V-3 assembly is a system in which six sodium channels are provided in the core of V-2 assembly so that the core is enlarged in its outside diameter to become critical. Therefore, it is not conceivable that V-3 is not different so much from V-2 in their nuclear characteristics. The discussion on the nuclear simulation of V-2 assembly and "JOYO" was already reported[2)] and therefore the simulation of V-3 assembly will not be discussed hereinunder.

This paper gives a report on the measurement and calculation of the reactivity worths of the B_4C simulating control rods in the V-3 assembly. Although V-3 is an engineering mock-up of "JOYO", it differs from "JOY" in the axial and radial blanket composition (the blanket in V-3 is composed of natural uranium metal while that in "JOYO" is made of depleted uranium oxide and sodium) and consequently the measured values * obtained on V-3 assembly cannot be used to estimate the corresponding values for "JOYO". A way to the estimation of the values on "JOYO" will be opened up by making use of the values obtained by corrective experiments and other experiments, such as the experiment for checking the degree of change of the measured values when the blanket composition is simulated, for instance. Or it would be possible to check the adequacy of the calculation method and group constants employed in the nuclear designing of "JOYO" by making a comparative study of the ratio of the theoretical to experimental values (hereafter referred to as "C/E") in such systems. Such discussion on C/E is particularly useful at a place removed from the center of the core.

In the engineering mock-up experiment, it is a matter of degree depending on the circumstances which of the above significances are to be given to the experimental system to be set up. Anyway, it is

---

* The simulating control rod is 1/2 of that of JOYO in weight and size.

essential to make clear what attitude be taken in planning the proposed experiment. For, when the former approach is used, the individual experimental values would be valueless unless the technical and theoretical methods of extrapolating the partial mock-up data into the full mock-up data are established and a consistent experimental plan is formulated.

The reactivity worths of the simulating control rods were measured at different positions in the core and with different number of the rods. Even the smallest was so large as exceeding 1 %δk/k that it is essntial to strictly define the reactivity in the experiment and calculation. In the present paper we assumed the reactivity of the system to be $1-1/k_{eff}$ when its effective multiplication coefficient is k_{eff} and defined the reactivity difference as the reactivity worth of what has caused such difference. That is to say that when the effective multiplication coefficient of the system has changed from k_{1eff} to k_{2eff}, the reactivity worth of what has caused the difference was obtained as $(k_{1eff} - k_{2eff})/(k_{1eff} \times k_{2eff})$.

Moreover, the reactivity change that has been caused in the system when the sodium channels were replaced with B_4C simulating control rods is called the simulating control rod worth.

There are several methods[3),4)] for measuring large reactivities and they can be classified broadly as; the critical method and the subcritical method. The critical method, which is employed for such purposes as the measurement of the central reactivity worth, is a method to know the reactivity worth of the unknown by reaching the criticality again by using the rod of known reactivity worth. In the case of the B_4C simulating control rod with a large negative reactivity worth, this method has the disadvantage that it requires a rod with a known large positive reactivity worth. Moreover, a system which has reached the criticality again with these rods have been inserted can be nuclearly different considerably from the original system.

The sub-critical method includes the neutron source multiplication method, the pulsed neutron method, the rod drop method, source jerk method, and the rossi- method. The reactivity worths of the B_4C simulating control rods on V-3 assembly were measured by use of the neutron source multiplication method, the pulsed neutron method, and partially by the critical method due to the restrictions arising

from the machine and the allowed period of experiments. This paper gives a report on the measured values obtained by use of the neutron source multiplication method and the calculated values. The results of experiments in which other methods were used will be reported in separate papers.

In the neutron source multiplication method, if the neutron source distribution is not the fundamental mode of the system, the higher harmonics of neutron flux will be excited and consequently it is not sure that the measured effective multiplication coefficient is the first eigenvalue of the system. Since we used in our experiments the neutrons produced by the spontaneous fission of plutonium in the fuel as the neutron source, the neutron source was uniformly distributed within the core. The insertion of the B_4C simulating control rod excites the higher harmonics to form an extremely asymmetric neutron field. In our preliminary measurements, we set up the detectors at different points to check the dependency on position of the effective multiplication coefficients and the reactivity worths of the system to be observed with the result that we found that there was a tendency for the increased saturation at the positions more removed from the center of the core.[5)]

In the said measurements, many detectors were used and the values obtained by these counters were averaged to obtain the "measured value", which was very close to the above-mentioned saturated value. When the B_4C simulating rods were so moved as they were arranged symmetrically about the center of the core, they ought to have the same reactivity worth but the different counters show different values. This problem was solved by obtaining the above-mentioned average value. However, there is no positive evidence that our measured value is the first eigenvalue of the system and a study is still under way on the systematic errors other than the errors of measurements arising from the variations in the detection efficiency and the counting rate and they are problems which are left to be solved in the future.

With regard to the different experimental systems in which the control rod positions were changed and different numbers of the rods were used, we obtained the effective multiplication coefficient by making calculations, using the multi-group diffusion code. It has been proved that the calculated value of the effective multiplication

coefficient is the first eigenvalue of the system, excluding the errors arising from the group constants and diffusion approximation.[6] This being so, the measured value can be compared directly when it is assumed that it is equivalent to the first eigenvalue of the system. If a sub-critical system of 1 %δk is to be known with an accuracy of 1%, k_{eff} must be calculated accurately down to 10^{-4}. In actuality, however, the calculated value normally is deviated about 1% from critical when the system is in a critical state.* Therefore, the comparison of the eigenvalues with one another will probably not produce very good results. However, to know the variations arising from the insertion of the B_4C simulating control rod is to take the difference between the two calculated values, thereby cancelling the systematic errors contained in k_{eff} of calculated values and therefore it must be calculated so reliably as to the place of 10^{-4} but it is not necessarily required for the value to be a real value down to 10^{-4}. On the other hand, it is necessary that a comparison of values based on the same physical concepts be made between the experimental and calculated values. From this standpoint, the aforesaid definition of reactivity worth was used.

When the calculated value was obtained for the purpose of accurately determining the variations thereof, we can be optimistic about the systematic errors but it is necessary to pay attention to the inclusion of variations arising from the causes other than those which actually caused the variations, e.g. errors of numerical calculation. It cannot be said definitely that the systematic errors of the calculated value has absolutely no effect on the variations. For example, if the SN calculation method is used, it will not only make more accurate calculations of the changes in the neutron flux distribution in the sodium channel and B_4C simulating control rod but also make a different evaluation (from the diffusion calculation method) of the changes in the leaking of neutrons from the core as the control rod is inserted. When using the effective cross-section, taking into consideration the heterogeneity (i.e., being composed of plate-shaped material) of the system, calculation is made of the neutron transport different from simple homogeneity calculation and

* In addition to the disagreement ascribable to the calculation method such as the diffusion approximation and the group constants, the disagreement between the experimental system and the calculation system is included.

it is expected to have an influence on the interaction effect and the like. In the present paper, however, no consideration is given to such effects but homogeneity calculation was used excluding the B_4C simulating control rods.*

Generally speaking, to different approaches are conceivable in making a comparative study of the experimental and calculated values. Firstly, calculations are made on a system which has been made in an appropriate model and thus obtained values are compared with the experimental values and the model is evaluated by the differences between the experimental and calculated values. In this case, the experimental values must be regarded as being absolute or else the standard for evaluation will be lost. The second is an attempt to faithfully reproduce the experimental system by calculations, thereby the adequacy of the group constants and the calculation method is checked or a check is made of the consistency of the experimental values by the verified group constants and the calculation method in order to make an evaluation of the experimental method. In the present paper, the second approach was employed.

As was discussed above, the comparison of the experimental and calculated values is inevitably made in the form of reactivity worth. What is obtained by the neutron source multiplication method is the effective multiplication coefficient of the system but in the process of data processing it goes to and from the reactivity and effective multiplication coefficient of the system.** Such being the case, the actual measured values are the values obtained through the calculated kinetic parameters. For this reason, there must be a consistency between the calculation of the kinetic parameters and the calculation of the values to be compared with the experimental values with regard to the reactivity worth. This is important in checking the group constants by experimental analysis. In the present paper, we used JAERI-FAST version 2[7] as the cross section set in all calculations.

This paper was compiled because we had established the experimental values by the neutron multiplication method and completed the two-dimensional diffusion calculation in all cases. We placed emphasis on the checking of the tendency and consistency of the ratio of the calculated to experimental values, thereby making efforts to

* Refer to Chapter 4.
** Refer to Chapter 3.

pick up the problems with the calculated values.

The reactivity worth of a material is preceded by the system on which it was measured and we will show the nuclear characteristics of the system principally in relation to the critical experiment of V-3 assembly and make reference to the dimensional comparison with "JOYO" in Chapter 2. Chapter 3 will deal with the experiments using the neutron multiplication method and the processing of the data derived from the experiments and the B_4C simulating control rods and the measurements of their reactivity worths. The calculation flow and the calculated values of the reactivity worths are shown in Chapter 4. In Chapter 5 is made a study on C/E, taking into consideration the various corrections enabling direct comparison of the measured and calculated values. The conclusion and the problems to be solved in the future are discussed in Chapter 6.

2. FCA V-3 Assembly

2.1 An outline of FCA V-3 assembly

The FCA V-2 assembly which was designed as the physics mock-up core of "JOYO was described in a previous given report.[2)]

The V-3 assembly has been designed as the engineering mock-up core of "JOYO" and it is exactly the same with V-2 assembly in their blanket and control/safety rod composition,[note)] but it is slightly larger than V-2 because it is provided with six channels for "JOYO" simulating control/safety rods. The simulating control rod channel is equivalent in size to an FCA matrix tube and the six control rod channels are located at equal intervals on a circumference of 23.4cm in diameter centering around the center of the core. Since the V-3 core has an average critical diameter of 35.4 cm while that of "JOYO" is 36.6 cm and the "JOYO" control/safety rods are located on a circumference about 21.6 cm from the core center, it may be said that the positions of the control safety rods of the V-3 assembly we have composed very well simulate those of "JOYO".

In the present measurements a system which has reached criticality with the simulating control rod channels being filled with sodium was regarded as a reference system because we were to measure the reactivity worth of the B C simulating control rod with sodium as a basis. We call the reference system the "clean core".

The following quantities would be of some help in obtaining a general idea of the characteristics of this "clean core".

$$k \fallingdotseq 1.8$$

$$mfe \fallingdotseq 200 \text{ keV}$$

The atomic number densities of the cores, blankets, sodium channels and B_4C simulating control rod channels are given in Table 1.

2.2 Critical approach

At the 0 step at the starting point of the near critical, the core drawers at the positions of the six simulating control rod channels each on the movable and fixed sides of V-2 assembly were replaced with the drawers filled with sodium. At the 1st step, 25

Note) Refer to Appendix (A1).

Table 1 Atomic number densities (10^{22} cm^{-3})

Nuclied	Core			Blanket			Na-channel		B_4C Control rod (Hcmogeneous)			B_4C Control rod (Heterogeneous)			
	V-3	JoYo	V-3C/R	V-3	JoYo-R	JoYo-Z	Plate	7-pin	7-pin	1-rod	JoYo	7-pin		1-rod	
												B_4C region	Na region	B_4C region	Na region
Pu-239	0.10458	0.10928													
Pu-240	0.009325	0.03905													
Pu-241	0.001069	0.00781													
U -235	0.1470	0.1665	0.4900	0.02891	0.00279	0.00219									
U -238	0.5836	0.5505	1.9453	3.9890	1.100	0.8619									
O	1.3101	1.7290			2.206	1.728									
Na	0.8134	0.9212			0.7304	0.9212	1.6592	1.5885	1.0830	1.0183	1.280		1.3047		1.3001
Al	0.8830		1.2502												
Cr	0.3273	0.3565	0.3805	0.1827	0.3086	0.3565	0.4065	0.4694	0.4708	0.4653	0.3752		0.6032		0.5941
Fe	1.1950	1.1610	1.3840	0.6652	1.006	1.1610	1.4936	1.6781	1.6925	1.6727	1.223		2.1686		2.1357
Ni	0.1535	0.1993	0.1642	0.07964	0.1727	0.1993	0.1752	0.1982	0.1988	0.1965	0.2100		0.2547		0.2509
Mo		0.0254			0.0220	0.0254					0.02676				
Mn								0.0196	0.0197	0.0193			0.0252		0.0246
B - 10									2.1198	2.0912	2.189	9.6565		9.6466	
B - 11									0.2314	0.2283	0.1969	1.0541		1.0527	
C									0.5386	0.5314	0.5966	2.4535		2.4513	
							(NC_1)	(NC_2)	(BC_3)			(BC_2)		(BC_1)	

( ); 1-dimension calculation run name.

core drawers were added and ten 1/2 core drawers were added at the 2nd step to reached the criticality, when No.1 control rod was fully inserted and No.2 rod was inserted 337.28 mm and the output power was 0.5×10^{-6}A in the linear power monitor #6.

After calibrating the control rods at the 2nd step, we proceeded to the 3rd step where we made adjustments around the core to improve the symmetry of the core. This is what is called the "clean core", which was used as a reference system hereafter.

The fuel loadings at the various steps are given in Table 2 and the pattern of V-3 clean core is shown in Fig. 1.

Table 2 Fuel loading steps at critical approach of assembly V-3

Step number	Fixed half				Movable half				Integrated number of fuel drawers
	Na	C/R, S/R	Fuel		Na	C/R, S/R	Fuel		
			Full	Half			Full	Half	
0	6	4	99	12	6	4	98	12	209
1	6	4	111	12	6	4	111	12	234
2	6	4	111	17	6	4	111	17	239
3	6	4	111	16	6	4	111	16	238

2.3 Calibration of control rod

The control safety rods of V-3 are so arranged as shown in Fig. 1. As for the standard reactivity calibration, we used the reactivity worth of No.9 safety rod on the movable side from when it is withdrawn 30.00 mm to when it is fully inserted as was usually used. When a reactivity change of $+\rho_0$ is given to the critical state, the doubling time of the clean core is

$$T_D = (100.40 \pm 1.06) \text{ sec}$$

From the above, the period is calculated as follows.

$$T = (144.85 \pm 1.54) \text{ sec}$$

Using β_{eff} and λ_i which are discussed in Chapter 4, the following standard reactivity worth can be obtained by the inhour equation.

$$\rho_0 = (3.55_5 \pm 0.02_9) \times 10^{-4} \ \delta k/k$$

Only the errors of period measurement are considered for the above

error. The reactivity worth calibration curves of No.1 and No.2 control rods were measured by the substitution method with the standard reactivity as a scale. The results are shown in Fig. 2.

2.4 Critical mass of V-3 clean core

The clean core of V-3 is loaded as shown in Fig. 1 when it is in a critical state. The amount of fuels loaded in the core at this time are as follows.

Pu-239, 241 ; 92.57 kg
U-235 ; 140.94 kg

In order to make it possible to compare the experimental values with the calculated values, various quantities which are difficult to calculate were obtained by experiments and properly corrected. As for the state before the corrections are made, we considered a system in which the control/safety rods in the actually loaded state were replaced with the core drawers.

The amounts of fuels at this time are as follows.

Pu-239, 241 ; 95.68 kg
U-235 ; 130.99 kg

The system which has been given the corrections corresponds to a cylinder core with no gap between contacted surfaces. The following items were considered for making corrections.

(1) Excess reactivity
(2) Gap effect
(3) Effect of loading difference of control/safety rods
(4) Effect of the core boundary shape
(5) Heterogeneity effect of fuel loading

For comparison with the two-dimensional XY calculation which will be discussed later, there is no need for any correction to (4) effect of the core boundary shape. For the core boundary shape can be accurately taken into the X-Y calculation. The various correction methods will be briefly explained below.

1) From the No.2 control rod position of 346.16 mm at the critical point with an output current of 0.50×10^{-7}A of linear output power monitor #6, the excess reactivity for V-3 clean core is

$(8.58 \pm 0.01)\rho_0$

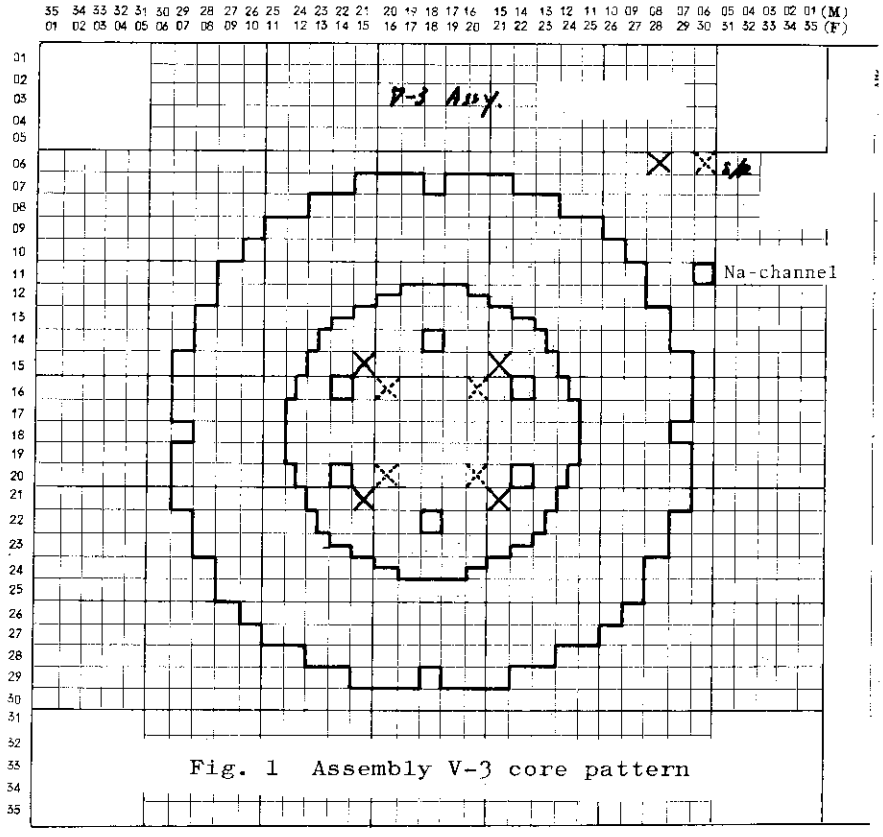

Fig. 1 Assembly V-3 core pattern

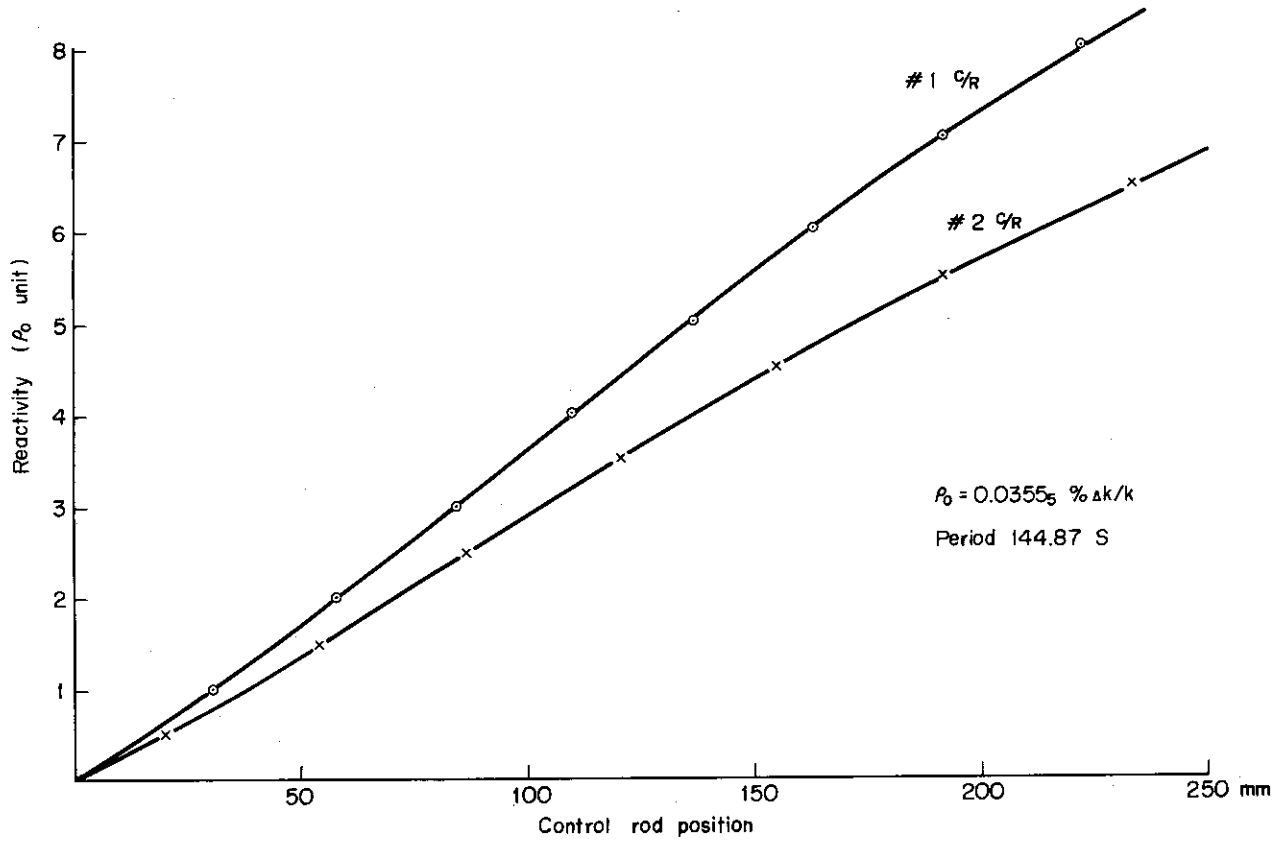

Fig. 2 Calibration curve of control rods of assembly V-3

2) With the assemblies on the movable and fixed sides in contact with one another, there is a gap of (2.6 ± 0.3) mm between the assemblies. So, from the control rod positions for the gaps between the 1/2 assemblies of 0.46 mm, 1.30 mm, 2.03 mm and 2.55 mm, the gap effect was obtained by extrapolation. The result was

$$(7.54 \pm 1.0)\ \rho_o$$

3) Next, we measured the effects of the control and safety rods. We made measurements when 16 - 20 on the fixed side was replaced with a dummy control rod and also when 15 - 21 on the movable side was replaced a dummy rod and found that the critical points in the two cases were 228.70 mm for No.2 control rod and 82.32 mm and 64.48 mm for No.1 control rod. Therefore, the amounts of correction for one rod were 2.92 ρ_o and 2.25 ρ_o on the movable and fixed sides, respectively, and the overall correction was

$$(20.68 \pm 0.20)\ \rho_o$$

We also measured the edge mass coefficient by attaching and removing the 1/2 core drawers of 12 - 21 on the movable and fixed sides. Thus obtained peripheral mass coefficient was as follows.

$$2.18\ \rho_o\text{-/rod}$$

4) In order to obtain the effect of the core boundary shape, the V-3 clean core irregularity becomes

$$W = \int_{\text{actual}} r \cdot ds - \int_{\text{ideal}} r_o \cdot ds = 0.61635$$

If the experimental value of $\partial\rho / \partial w$ in V-2 assembly, i.e. -0.1020%δk/k is used, the core boundary shape effect becomes

$$-(1.79 \pm 0.1)\ \rho_o$$

5) As for the heterogeneity effect, we used the following value measured on V-2.

$$(9.5 \pm 1.3)\ \rho_o$$

The above corrections are summarized in Table 3 and the critical mass and critical dimensions are given in Table 4.

Table 3 Corrections to the loaded mass

Item	Reactivity change (ρ_0 *)	Mass to be corrected (kg)	
		Pu-fissile	U-235
Excess reactivity	-(8.60± 0.01)	-(1.535± 0.002)	-(2.103± 0.002)
Effect of spiked S/R and C/R	+(20.04± 0.20)	+(3.52 ± 0.04)	+(4.90 ± 0.05)
Gap effect	-(7.54 ± 1.0)	-(1.35 ± 0.18)	-(1.84 ± 0.25)
Effect of irregular core boundary	-(1.79 ± 0.1)	-(0.320± 0.018)	-(0.438 ± 0.024)
Subtotal	+(2.1 ± 1.1)	+(0.37 ± 0.19)	+(0.51 ± 0.26)
Heterogeneity effect	+(9.5 ± 1.3)	+(1.70 ± 0.23)	+(2.32 ± 0.32)
Total	+(11.6 ± 1.7)	+(2.07 ± 0.30)	+(2.84 ± 0.41)

* $\rho_0 = 0.0355_5$ % k/k

Table 4 Critical parameters

	Critical mass (kg)		Critical dimensions		
	Pu-fissile	U-235	H(cm)	R (cm)	V (l)
Heterogeneous cylinder core	96.05 ±0.20	131.50 ±0.27	60.96	35.42 ±0.03	240.2
Homogeneous cylinder core	97.75 ±0.30	133.83 ±0.41	60.96	35.72 ±0.05	244.3

3. Experimental value of reactivity worth of B_4C simulating control rod by the neutron multiplication method

3.1 Experiments

3.1.1 Outline

The neutron source multiplication method is commonly used at critical approach and also used as a supplementary method in a case where a very high degree of accuracy is required. It is generally believed that the results obtained by this method are not so good in reliability. It is also said that the reliability of this method ranges to somewhere around $-2\%\delta k/k$.[4] In our experiments, it was necessary to make measurements up to $-8\%\delta k/k$ and a series of preliminary experiments were conducted to make a study on the relationship between the neutron flux detector positions and the sub-criticality to be measured.[5] This study was made by changing the position of the B_4C simulating control rod within the core. The details of these experiments will be discussed in another report.

As a result of the preliminary experiments, we found that as the detector is removed from the core, the sub-criticality to be measured showed a tendency to be saturated[note] and that the sub-criticality was reached faster in the direction between R and Z directions. It was also confirmed, that although indirectly, that as the B_4C simulating control rod is inserted, the reactivity worth of the FCA control rods and the gap effect of half machine change.

The defects of the neutron source multiplication method is ascribable to the space distribution of neutron sources. In our experiments, we used spontaneous neutrons of Pu fuel as the neutron sources. In the preliminary experiments, external neutron sources were used additionally to measure the sub-criticality of the system and in this case we observed a tendency for the sub-criticality to become several percents smaller. However, the FCA is so constructed that it is impossible to insert external neutron sources into the center of the core and the neutron source distribution presumably becomes more different from the pattern of the first eigenfunction. So, we did not use the external neutron sources in the present measurements.

Note) Refer to Appendix (A2).

We used ten detectors which were set up on the outside of the core and blanket. Care was taken that there was no movement of material between the assembly and detectors to avoid the changes in the detection efficiency during the experiment.

At the present time when the relationship between the detector positions and the sub-criticality to be observed is not analytically clarified, in order not to pick up peculiar values, we attached importance to the aforesaid saturating tendency and averaged the values measured by the detectors by applying adequate weight to them and took the mean value as the "measured value".

3.1.2 Fundamental principle of experiment

The fundamental formula in the neutron source multiplication method is as follows.

$$N = \frac{A}{1 - k_{eff}} \qquad (1)$$

where the symbols are usually used ones. It is understood that A includes the intensity of neutron source, the lifetime of neutrons in the system, and the neutron detection efficiency of the detectors. However, the system is actually described by the Boltzmann's equation.

$$L\phi = M\phi + S$$

This is used as the eigenvalue equation

$$L\phi = \frac{1}{k_{eff}} M\phi$$

The first eigenvalue of this equation is physically understood as the effective multiplication coefficient of the system.[6)]

In considering the relationship between these transport equations and equation (1), if the external neutron source S assumes the form of the first eigenfunction of the system, k_{eff} of equation (1) becomes the first eigenvalue of the eigenvalue equation and becomes the effective multiplication constant itself of the system. If the external neutron source is not distributed in the form of the first eigenfunction, it cannot be rearranged as equation (1). Even if the external neutron source S is distributed in the form of the first eigenfunction, it is impossible to experimentally know A unless the effective multiplication coefficient of the system is known. So, A

will be measured on a closely resembling system, of which the effective multiplication constant is known. Even in this case, if the first eigenfunctions of the two systems differ in form, it is impossible, strictly speaking, to apply the measured A to the system, of which the effective multiplication coefficient is unknown. Such being the case, it is inevitable for the present experiment to include systematic errors when the systems on which the neutron distribution and A are to be measured are deviated from the aforesaid principle.

In order to make experimental evaluation of the systematic errors, there are such conceivable methods as measuring A on several resembling systems or checking the variance of the subcriticality of the system to be observed at different places or slightly altering the neutron source distribution. However, it cannot be said that these methods are sufficient.

3.1.3 Experimental method

The flow of the whole experiments is shown in Fig. 3. As for the neutron source, we used the spontaneous neutrons of the Pu fuel in the core. There are methods of experiment. One of them in the "A Method" in which A is obtained beforehand in a known sub-critical system and then N in the unknown sub-critical system is measured to know the k_{eff}. The other is the "$\delta\rho$ Method" in which the k_{eff} of the unknown sub-critical system is known from the changes caused in N by adding the known reactivity $\Delta\rho$ in the unknown sub-critical system. The latter method has the advantage that there is no need to know A.

In our experiments, we followed the procedure as below. The known sub-critical system for the measurement of A was realized by raising the FCA control and safety rods (hereafter referred to as "S/R" and "C/R") which had been calibrated in a critical system. As for the calibration of S/R and C/R, we used the asymptotic period method in which time required for the output power to be doubled was obtained and it was converted into reactivity by using the inhour equation.

Next, when measuring N in the unknown sub-critical system in which B_4C simulating control rods are inserted, measurements were made with S/R and C/R being fully inserted or at different levels of

insertion for the purpose of making the sub-criticality as shallow as possible. Therefore, the k_{eff} of the system which was measured on the basis of equation (1) included the effects of replacement of sodium with B_4C simulating control rods and also of the changes in the positions of S/R and C/R and they required proper corrections. The process of calculation of the reactivity worths of B_4C simulating control rods from the masured values in the "A Method" and " $\delta\rho$ Method" will be discussed below.

(1) A Method

The measurement of A was made by withdrawing FCA S/R and C/R as was stated above. Since S/R and C/R were previously calibrated, the reactivity of the system at this time can be obtained and accordingly the effective multiplication coefficient k_{oeff} of the system can be obtained as follows.

$$k_{oeff} = \frac{1}{1 - \rho} \tag{2}$$

Therefore A can be obtained as follows from equation (1) by using the counting rate No of the detector in this sub-critical system

$$A = N_0(1 - k_{oeff}) = N_0(1 - \frac{1}{1 - \rho}) \tag{3}$$

Next, the effective multiplication constant k_{meff} in the unknown sub-critical system after B_4C simulating control rods were inserted becomes as follows from equation (1) by using the counting rate Nm of the detector at the time.

$$1 - k_{meff} = \frac{A}{N_m} \tag{4}$$

And the reactivity ρ m of the reactor at this time becomes

$$\rho_m = \frac{k_{meff}-1}{k_{meff}} \tag{5}$$

As was mentioned above, this ρ m includes the B_4C simulating control reactivity worth $\delta\rho_B$ and the additional reactivity ρ_a arising from the changes in the positions of FCA C/R and S/R before and after the replacement of sodium with B_4C simulating control rods. By assuming the additivity of the reactivity of the reactor

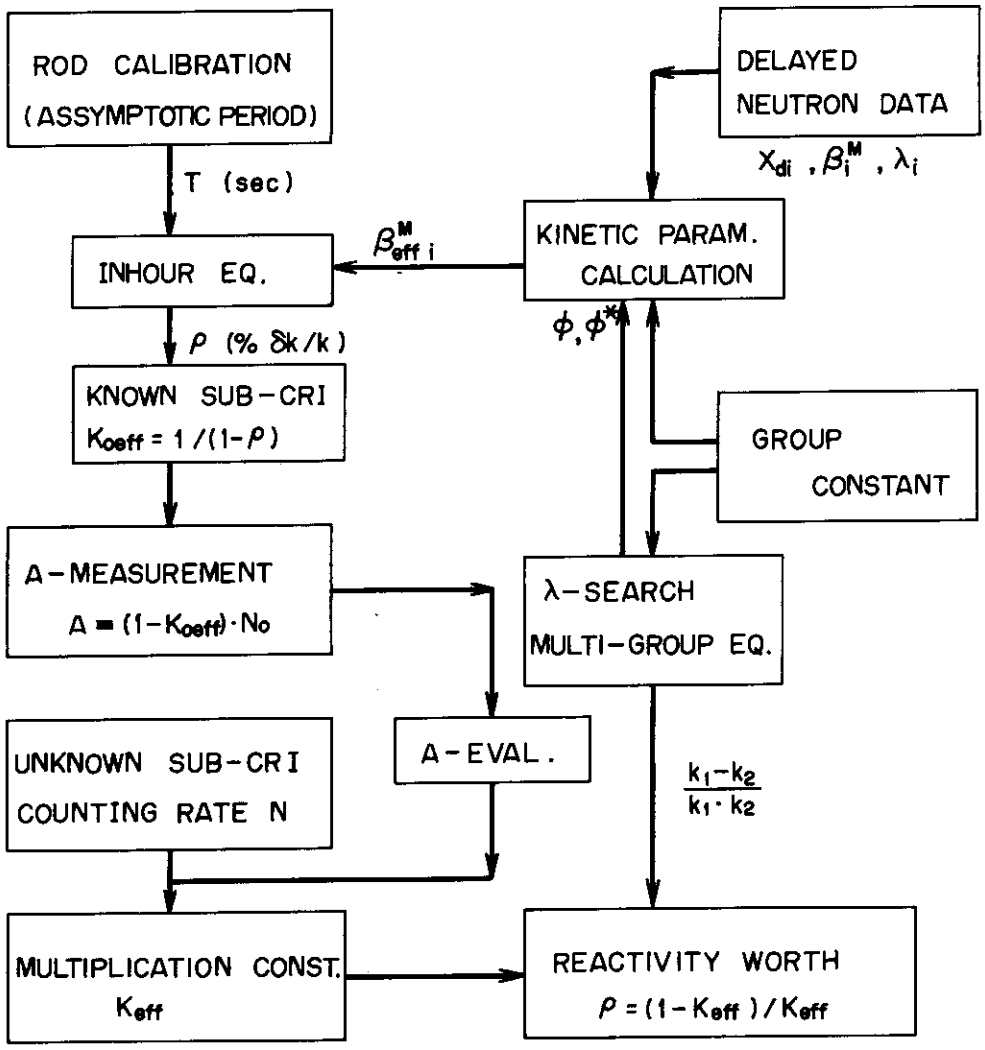

Fig. 3 Experimental flow (S.M method)

$$\delta\rho_B = \rho_m - \rho_a \tag{6}$$

Thus, the reactivity worth of B_4C simulating control rod is known. As for the additional reactivity ρ_a arising from the changes in the positions of C/R and S/R, we used the value at the critical time of the system, that is, before the B_4C simulating control rods were inserted. However, when the value of ρ_a is sufficiently small compared with $\delta\rho_B$, it may be considered that the above superposition does not become a large source of errors. As we have just discussed, what is obtained by the neutron source multiplication method is the effective multiplication constant of the system and when calculating the reactivity worths of the B_4C simulating control rods, we converted them into the reactivity of the system at different stages and superposed the additivity with regard to reactivity.

(2) $\Delta\rho$-Method

From equation (1) the k_{1eff} in an unknown sub-critical system is

$$1 - k_{1eff} = 1 - \frac{1}{1-\rho_1} = \frac{A}{N_1} \tag{6}$$

When the known reactivity $\Delta\rho$ is added to this system

$$\rho_2 = \rho_1 + \Delta\rho \tag{7}$$

$$1 - k_{2eff} = 1 - \frac{1}{1-\rho_2} = \frac{A}{N_2} \tag{8}$$

From equation (6) and (8), the reactivity ρ_1 of the first unknown sub-critical system becomes as follows by using $\Delta\rho$ and the counting rates N_1 and N_2.

$$\rho_1 = \frac{1}{2}\left\{(1-\Delta\rho) - \sqrt{(1-\Delta\rho)^2 + \frac{4N_2}{N_2 - N_1}}\right\} \simeq - \frac{N_2}{N_2 - N_1}\ \Delta\rho \tag{9}$$

In our experiments, N_1 was counted in the unknown sub-critical system in which the B_4C simulating control rods were inserted and then N_2 was counted by moving properly the FCA S/R and C/R to add $\Delta\rho$ and ρ_1 was obtained from equation (9). $\Delta\rho$ is obtained from the calibration curve at the critical time. The calculation of the reactivity worth of B_4C simulating control rod from ρ_1 is the same as in the case of the A Method.

In this method, there is no need for obtaining the value of A and for this reason the experiment can be completed in a shorter time and is easier than the A Method with regard to the variations in the efficiency of the detectors. However, as is clear from equation (9), the errors of $\Delta\rho$ becomes those of ρ_1 and there is a big problem in using the value before the insertion of B_4C simulating rods for $\Delta\rho$. And the experimental error of the quantity of the difference $N_1 - N_2$ also cannot be ignored.

The experimental data were processed in the A Method and the $\Delta\rho$ Method. The $\Delta\rho$ Method always produced larger reactivity worths than the A Method. It was clear that $\Delta\rho$ changed due to the insertion of B_4C simulating control rod in other supplementary experiments. Such being the case, we decided to adopt the value obtained by the A Method as the reactivity worth of B_4C simulating control rod.

3.1.4 Measuring system

We prepared ten measuring systems for counting the neutrons. Of these systems, four were FCA nuclear monitoring systems and the other six were newly installed. The masuring circuit system is shown in Fig. 4. All the counters were covered with 20 cm to 30 cm thick polyethylene or paraffin in an attempt to increase the counting efficiency.

The positions of the counters are shown in Fig. 5 and their distances from the core center in Table 5. All the counters were located outside the core and blanket and measured the leaking neutrons. Such being the case, care was taken that there arise no changes in the leaking conditions other than the replacement of sodium with B_4C simulating control rods. When the FCA control rods are withdrawn, the blanket is also moved outward and therefore these control and safety rods were surrounded with natural uranium metal from the back end of the lattice tube to protect the counters in the Z radial direction from being directly influenced by the movements of the control and safety rods.

The dead time of each counter was measured by a synchroscope and by varying the reactor power output at the critical time. As for the background of neutrons, it was practically impossible to make measurements because it was necessary to take Pu out of the

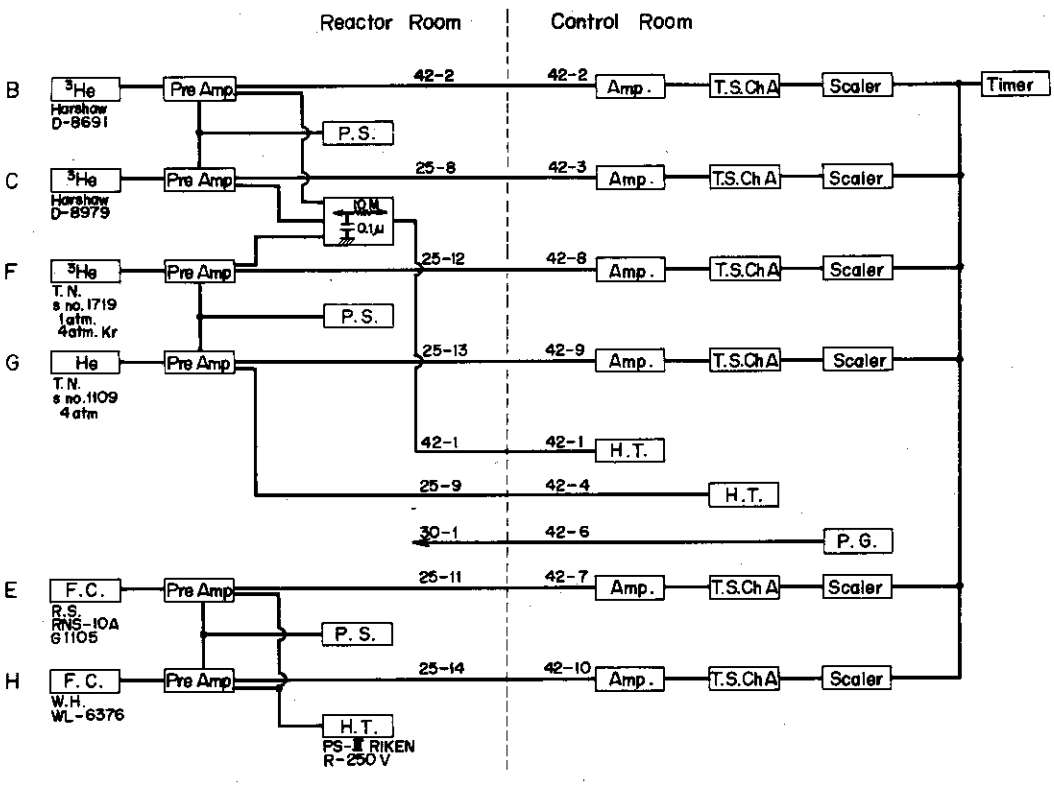

Fig. 4 Counting system block diagram

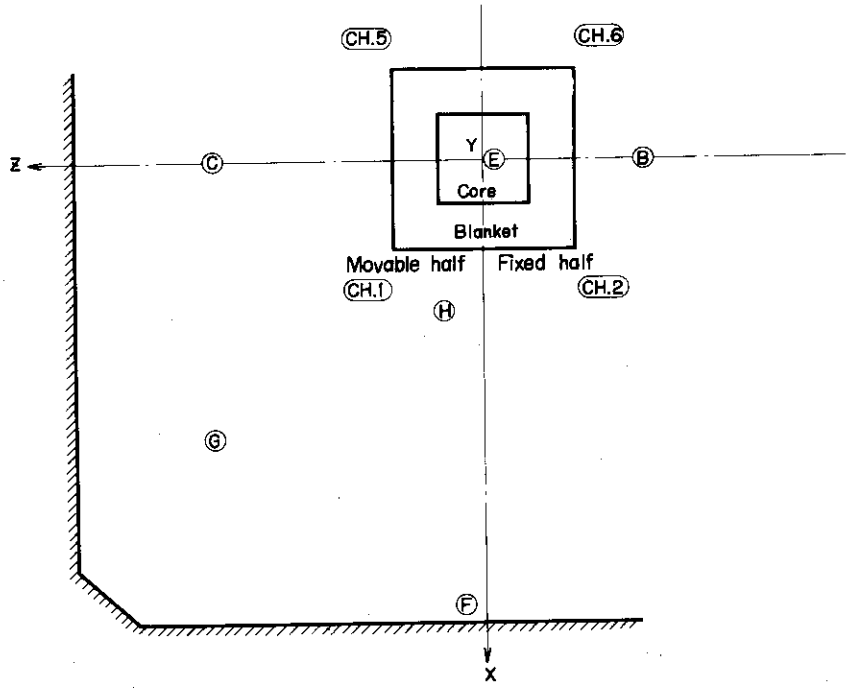

Fig. 5 Counter position for source multiplication measurement (observed from the top of the assembly)

reactor room. We decided that there was no need of considering the neutron background, judging from the performance inspection data on the external neutron sources when loaded and the data measured by the radiation monitor when the uranium core was used. The noise coming into the circuit system was separately measured but it was ignored because it was negligibly small. The evaluation of the dead time of the counter is required in measuring A and the evaluation of the neutron background is needed in measuring N of the distant counters in a deep sub-critical system.

3.1.5 Averaging of measured values

As was discussed above, ten counters were used to obtain the values of A and N and therefore 10 values of reactivity worth were obtained at one time. These values were averaged as follows. As for the weights in the averaging procedure, the measuring accuracy of the respective counters must be considered first of all. The measuring accuracy is better for the counters with higher counting rates. From this it follows that larger weights are applied to the counters nearer to the core. The increase and decrease of the whole neutrons in the core is important from the standpoint of knowing the reactivity of the reactor and the weights with regard to the positions of the counters are also needed in order to view the inside of the core as evenly as possible. Here we thought it in the simplest way so that the square of R, the distance from the core center to the counter, was used as a weight. The variations in the average value due to the difference in weighting method are not large and example is shown in Appendix (A3). The averaging procedure was done at the stage where the reactivity of the system was obtained. By this, it is also possible to obtain the average value of the reactivity worths.

3.2 B_4C simulating control rod

3.2.1 Simulating control rod

The "JOYO" B_4C simulating control rod is composed of Calandria and fuel pins (or rods) and has an overall size of 300mm × 50mm × 50mm so that it may be contained in the FCA drawer. The Calandria are of two types: one contains 7 pins and the other 1 rod and they are called the "7-pin cluster type" and "1-rod type". The pin or

rod contains sodium, natural B_4C and enriched B_4C ($90\%B^{10}$).

The 7-pin cluster type was used mainly in our experiments and this paper gives only the experimental and calculated values with regard to this type.

The Calandria of the 7-pin cluster type is illustrated in Fig. 6(a) and the dimensions of the Calandria and pin are given in Table 6.

The Calandria is constructed with SUS27 plates and contains sodium. The pin is made of SUS27 and is tubular in shape.

The B_4C contained in the pin (SUS tube) are in the form of 11.0mm ×12mm pellets formed by sintering. A SUS tube filled with the pellets makes a B_4C pin. The chemical composition and the isotope ratio of the enriched B_4C are shown in Table 7. The data were provided by PARTIOT, the manufacturer of the B_4C pellets and from which we calculated the atomic number density we used in our calculations.*

When this simulating control rod is handled in nuclear calculations, two models, homogeneous and heterogeneous, are used. The homogeneous model is a model in which the Calandria and pins, including FCA lattice tubes and drawers, and their contents are assumed to be present in a mixed state in a space of 55.2mm × 55.2mm × 304.8mm. In the heterogeneous model, the shape of the Calandria was approximated to a circle with such diameter as to have an equivalent area as illustrated in Fig. 6(b). In order that the B_4C singularity may be calculated faithfully, the diameter of the actual B_4C pellet was used for the diameter of the B_4C region. The sodium region was made into a model, assuming that the SUS of the FCA lattice tubes, drawers, Calandria and pins, and the sodium in the Calandria are homogeneously mixed. The isotopic densities in the homogeneous and heterogeneous models are given in Table 1.

3.2.2 Comparison with "JOYO" control rod

The aforesaid simulating control rod is about 1/2 of the "JOYO" control rod in the B^{10} weight, that is, 655 g per one rod against 1,162 g. The pin for the simulating control rod are thinner (11.0 against 15.2) and the pin pitch is narrower (16.1 mm against

* The Partiot's measuring accuracy is about ten times better than the domestic one.

Table 5 Counter positions represented by X, Y and Z coordinates and their distances from core center

Counter	X-coordinate cm	Y-coordinate cm	Z-coordinate cm	Distance from core center cm
B	0	0	-194.4	194.4
C	0	0	423.3	423.3
F	687.8	-44.2	20.0	689.5
G	467.8	-137.6	375.0	615.1
E	0.0	-71.8	0.0	71.8
H	169.8	-144.6	90.0	240.5
CH1	82.8	71.8	86.0	139.3
CH2	82.8	71.8	-86.0	139.3
CH5	-82.8	-93.8	86.0	150.2
CH6	-82.8	-93.8	-86.0	150.2

The origine of the coordinates lies at the core center.

Table 6 Mock-up control rod specification

		Pin		Rod	Calandria		
		ETL	ETS		L7	S7	L1
Weight gr	B_4C	67.23±0.18	33.58±0.05	464.25±1.36			
	SUS	54.25±0.13	30.59±0.05	367.05±0.07	845.8±0.8	473.	834.5±0.5
	Na				361.0±2.6	183±1	361
Length	mm	308.2	158.2	308.1	309.94	159.95	309.85
B_4C length	mm	300.45	150.38	300.90			
Outer dia.	mm	12.50	12.50	33.06			
Inner dia.	mm	11.44	11.49	30.34			
B_4C dia.	mm	11.03	11.03	29.0			
Pin pitch	mm				16.11	16.11	

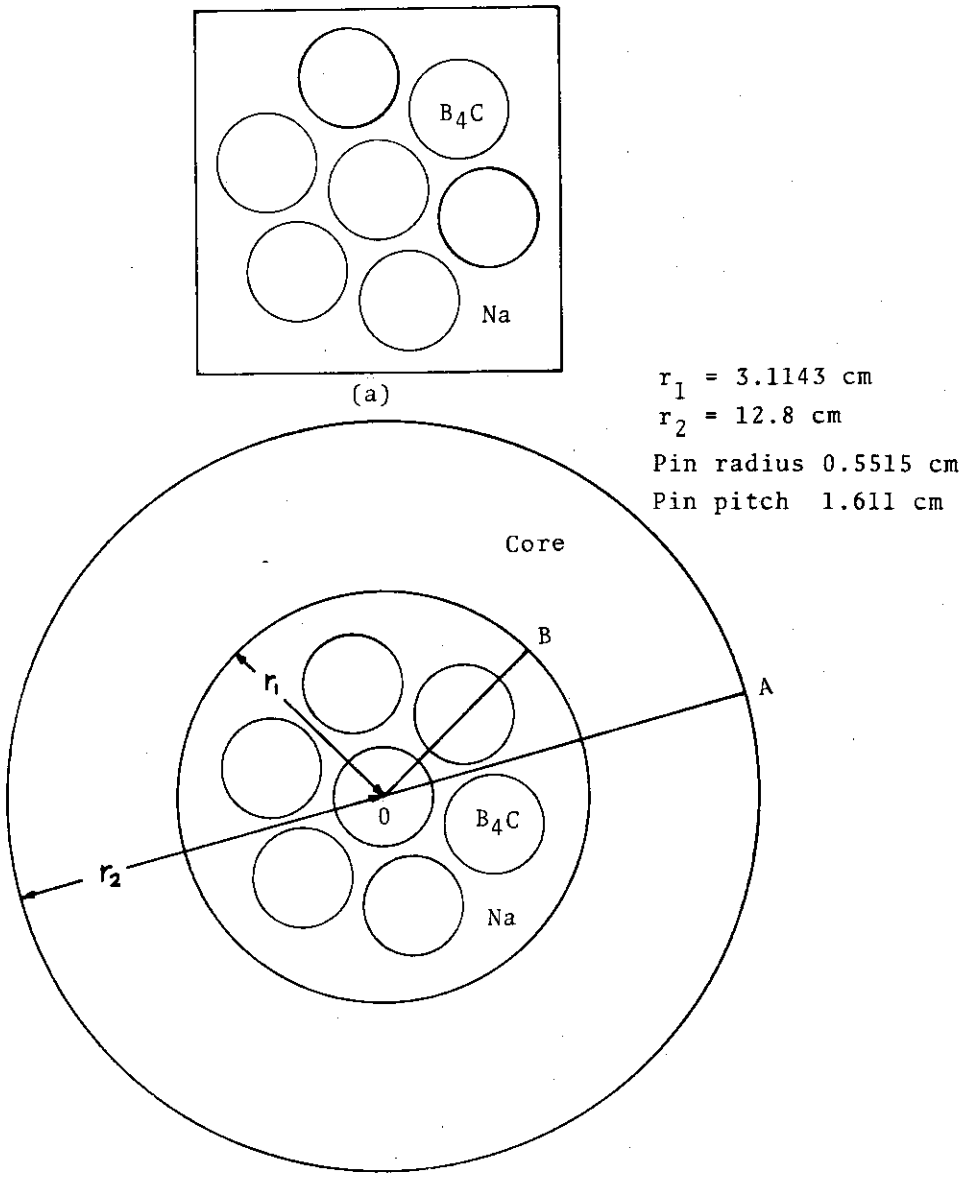

Fig. 6 Cluster type B_4C rod arrangement for effective cross section calculation by Collision probability code PIJF & CLUP

Table 7 Chemical analysis of B_4C pellet (Partiot)

Boron	77.9 %
C	21.2 %
Fe	0.13 %
Si	0.20 %
Al	0.05 %
B_2O_3	Less than 0.1 %
Ti, Cu, Mn, Na	Less than 100 ppm
Cl + F	Less than 100 ppm
Co	Less than 50 ppm

Boron istopic analysis; B^{10}= 90.16±0.02%

19.7 mm) and consequently the outside dimensions are smaller than the "JOYO" control rod. The average density of B^{10} is higher in the simulating control rod (0.353 gr/cc against 0.337 gr/cc). The isotopic densities of the "JOYO" control rods are given in Table 1.

3.3 Experimental results

3.3.1 Experimental values

The sodium channel drawer is composed of the sodium pins and Calandria up to the core height (6 × 5.08 cm) and its blanket is made of natural uranium metal like other blankets. The B_4C simulating control rod is composed of B_4C pins and Calandria up to the core height and its blanket is also made of natural uranium metal. The reactivity changes arising from the replacement of these two on the fixed and movable sides were used as the reactivity worths of the B_4C simulating control rod drawer is restricted to the B_4C 7-pin cluster type. The reactivity worths in the cases of the one-rod type, plate type and natural B_4C* are not discussed in this paper but clearly stated when they are referred to in some exceptional cases.

As was described in 3.2, the B_4C pin is wrapped up with SUS and when it is loaded in the drawer a SUS pressure plate is used on its front surface. This being so, when the B_4C simulating control rod drawer is loaded in the core, there occurs a gap at the front surface of the B_4C simulating control rods on the fixed and movable sides. The gap width is as follows.

Rod plug	0.36 cm (SUS)
Pressure plate	0.08 cm (SUS)
Drawer front face plate	0.08 cm (SUS)
Gap between contact surface	0.05 cm (Air)
Total	0.57cm × 2 = 1.14 cm

The experimentally obtained reactivity worths of B_4C simulating control rods, together with the names and positions, are given in Table 8. These experimentally obtained values of reactivity worth are not given the corrections with regard to the above-mentioned center gap. In 4B and 5B experiments, a one-rod type B_4C simulating control rod was used at the position of 20 - 22 and 16 - 22,

* Refer to 3.2.

respectively but the obtained values were converted into the values in the case in which 7-pin type B_4C rods were used. The conversion coefficient which was used for this purpose was

$$\delta\rho(\text{one-rod type}) = 0.908\delta\rho \ (\text{7-pin type})$$

This value was calculated from the measured reactivity worth of each of the two types of B_4C rods in the core center of FCA V-2 assembly. Further details will be discussed in a separate paper.

Each experiment will be explained according to Table 8. The core pattern in each experiment is shown in Fig. 7.*

(1) 1 B experiment (B1, B2, 1BC)

The reactivity worth of a B_4C simulating control rod was measured at different points in the core. In the case of 1BC, we measured the reactivity changes arising from the replacement of the 18 - 18 sodium channel is the center with B_4C simulating control rod. At this time, A was the value when 18 - 18 was the sodium channel. In order to measure this A, criticality was reached by replacing the peripheral sodium chennels of F14 - 18 and M22 - 18 with the fuel drawers (SEU) containing 20% enriched metal uranium.

(2) 4B and 5B experiments

In the cases of B1 and B2, the system is so low in sub-criticality that the deviation of the values of sub-criticality according to the counter positions is less than 1% but when there are so many rods as in 4B and 5B, the deviating of the measured values of sub-criticality appears noticeable. This phenomenon is mainly responsible for the experimental errors.

(3) Tr experiments (Tr-1, Tr-2, Tr-3)

This is a series of experiments on the radial traverse of the reactivity changes when two B_4C simulating control rods positioned symmetrically from the core center have replaced the sodium channels. In all the experiments, we used the value of the V-3 clean system for A. There was no trouble in Tr-1 but it was not appropriate in other experiments. This will be discussed in Chapter 5.

---

* Refer to 4.1.8, for Q, H and F at the names. In Pa-series, the numbers of sodium channels are different between experiments and calculation.

Table 8 Rod position and reactivity worth by source multiplication method

Experimental No.		Mock-up control rod position							Rod worth ρ_o	Rod worth % $\Delta k/k$
		14-18	16-14	16-22	20-14	20-22	22-18	Other positions changed		
1B-	1BC	Na	Na	Na	Na	Na	Na	18-18 ; MCR	70.8 ±1.2	2.52±0.04
	B1	Na	Na	MCR	Na	Na	Na		31.37±0.37	1.12±0.01
	B2	MCR	Na	Na	Na	Na	Na		37.06±0.37	1.32±0.01
4B,5B-	4B	Na	MCR	MCR	MCR	MCR	Na		126.6 ± 2.0	4.50±0.07
	5B	MCR	MCR	MCR	MCR	MCR	Na		164.7 ± 2.8	5.86±0.10
Tr-	Tr-1	MCR	Na	Na	Na	Na	MCR		76.6 ± 1.0	2.72±0.04
	Tr-2	ND	Na	Na	Na	Na	ND	15-18, 21-18 ; MCR	100.6 ± 1.1	3.58±0.04
	Tr-3	ND	Na	Na	Na	Na	ND	16-18, 20-18 ; MCR	117.2 ± 1.7	4.17±0.06
In-	In-1	MCR	Na	Na	Na	MCR	Na		69.91±0.88	2.49±0.03
	In-2	MCR	Na	MCR	Na	Na	Na		67.87±0.92	2.41±0.03
	In-3	Na	Na	MCR	Na	MCR	Na		59.28±1.67	2.11±0.06
Pa-	Pa-1	MCR	Na	ND	ND	Na	Na	14-19; MCR, 22-17; Na	58.61±1.0	2.08±0.04
	Pa-2	MCR	Na	ND	ND	Na	MCR	14-19; MCR, 22-17; MCR	124.2 ±2.2	4.42±0.07

Na ; Na drawer, ND ; normal drawer, MCR ; mock-up control rod

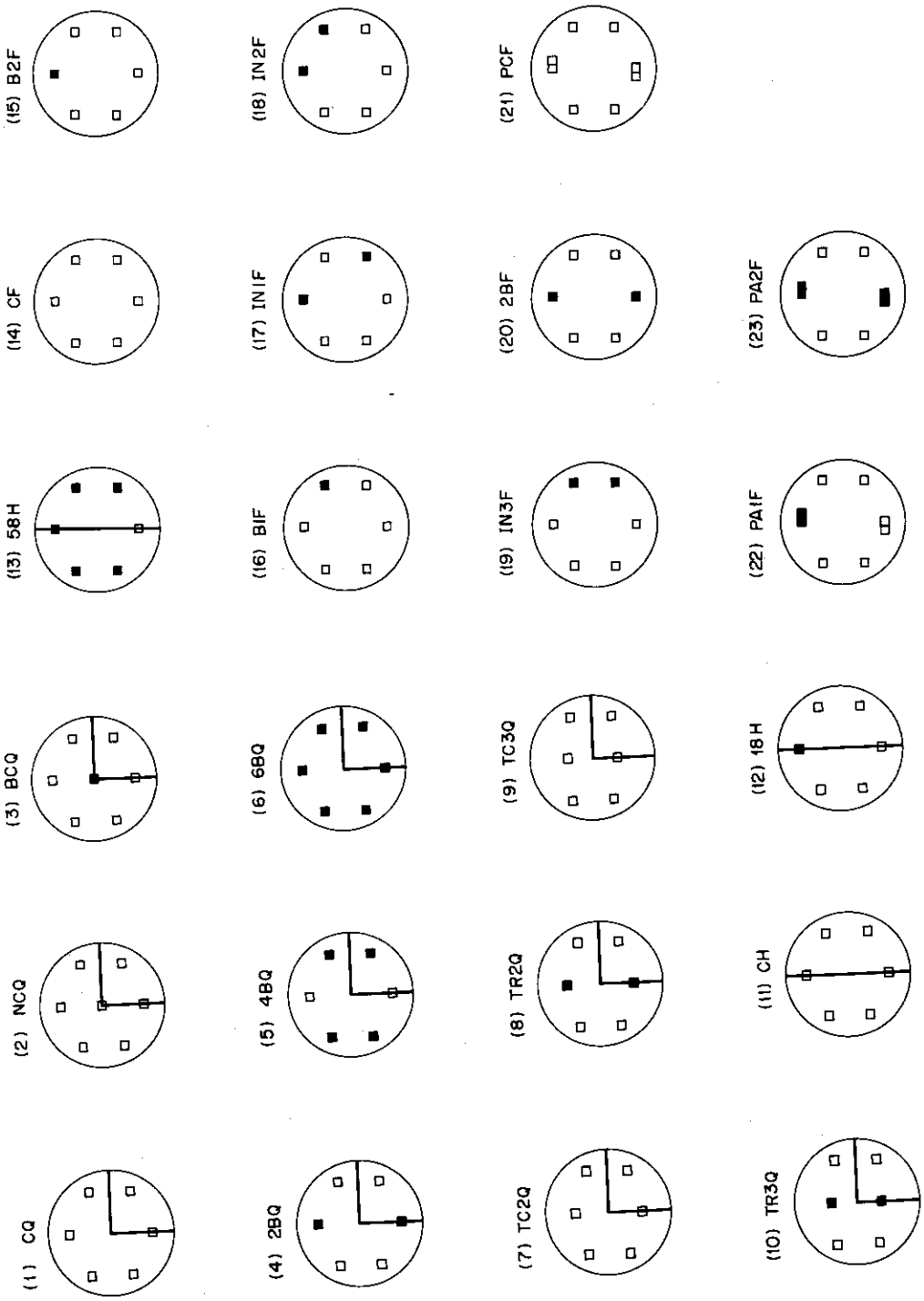

Fig. 7-1 B_4C control rods loaded core pattern

Fig. 7-2 B_4C control rods loaded core pattern

(4) In experiments (In-1, In-2, In-3, Tr-1)

This series of experiments were conducted to investigate the interaction when two B_4C simulating control rods were inserted in the core. The asymmetry is emphasized depending on the core pattern and it is reflected in the experimental errors. Tr-1 is naturally also the data relating to the interaction.

(5) Pa experiments (Pa-1, Pa-2)

In these experiments a pair of adjacent B_4C simulating control rods inserted in the core was regarded as a single rod and its reactivity worth and interaction were measured. A was measured with the sodium channels of 16-22 and 20-14 were replaced by 14-19 and 22-17 fuel drawers and thus obtained value of A was used in these experiments. When compared with B2 experiment, Pa-1 resembles it in its core pattern but the error increased with the increase of singularity. The two simulating rods were placed close to each other simulating the arrangement of control rods in "JOYO".

3.3.2 Experimental accuracy

As for the random error sources for the experimental values, such factors as the variations in the neutron counting rate, uncertainty of the FCA control rod positions, and the degree of contact. However, the last factor was ignored because it is sufficiently small as compared with the finally obtained reactivity worth of B_4C control rod. As for the variations arising from the counting of neutrons, the counting was made repeatedly to obtain the standard deviation. In calculating the reactivity of the system with regard to the counters, the above two factors were adopted in accordance with the law of error propagation to determine the errors in the reactivity measured by the counter. In the averaging operation, we obtained the standard deviation of ten measured values and the above-mentioned erros were employed as the weights used in the averaging operation. Thus obtained standard deviation is an average value of the errors in the reactivity measured by the counters.

A of V-3 clean system was measured several times during the experiment. The variations in reactivity of the system which were measured by using the value of A obtained in such different

measurements were within the aforesaid standard deviation in some cases but generally they exceeded the standard deviation, although rarely exceeded two times the standard deviation. Since there were no re-measurement data for N, the reactivity was finally determined by the average value of reactivities with different A and its error was made 2 times of the variations around the average value of the reactivity measured by using the different values of A. As for the errors of the patterns for which no re-measurements of A were made, they were obtained by doubling the standard deviation of the average value for the ten counters.

The causes of systematic errors were referred to in 3.1.2. When the average value for many counters located in different positions is taken to obtain the standard deviation, some of the systematic errors will probably be taken in. However, no attempt is made in this paper to consider what is clearly called the systematic errors as experimental errors.

3.3.3 Interaction effect

We calculated the interaction factor, using the data of In-experiment and Tr-1 experiment. The results are given in Table 9. The interaction factor is defined as follows.

$$f_{ij} = \frac{\delta\rho(i,j)}{\delta\rho(i)+\delta\rho(j)}$$

where $\delta\rho(i)$ and $\delta\rho(j)$ are the reactivity worth of a B_4C simulating rod at positions i and j, respectively, and $\delta\rho(j,j)$ is the reactivity worth when the two simulating control rods are inserted in i and j positions at the same time.

Table 9 Interaction factor f_{ij} by source multiplication method

Exp. No.	positions		angles	distance (cm)	f_{ij}
	i	j			
In - 3	16-22	20-22	50°	22.08	0.972 ±0.016
In - 2	14-18	16-22	65°	24.69	0.993 ±0.011
In - 1	14-18	20-22	115°	39.81	1.022 ±0.011
Tr - 1	14-18	22-18	180°	44.16	1.034 ±0.011
Pa - 2	14-18	22-17	180°	44.16	1.060 ±0.013
	14-19	22-18			

angle: observed at core center

Roughly speaking, the denominator and numerator offset each other for A in the calculation f_{ij} and therefore the error can be considered to be less than twice the standard deviation of the average value of 10 counters with a certain A. Such being the case, it becomes a relative error of about 2^{-1} of the reactivity worth of a B_4C simulating control rod as shown in Table 8. No attempt is made to adopt systematic errors in any definite form in this case, too.

Looking at Table 9, it is seen that the interaction between the two B_4C simulating control rods show the reversal of the interaction in direction at 90° around the core center and reaches the peak at 180°, that is, when they are on a diagonal line. The Pa-experimental data show that the intensity of interaction depends on that of singularity and changes in proportion to the latter.

3.3.4 Discussion on the experiments

The interaction between the two B_4C simulating control rods was discussed in the preceding paragraph. We found that the additivity depended on the relative positions of them.* In the case of 5B experiments, for example, it is 1.013. From this, it is known that when distributed so symmetrically the additivity of reactivity at least with regard to the absorber was maintained as far as a considerable sub-critical system. However, this will not directly enhance the reliability of the absolute values of the experimental values. There are problems about the application of A.** A question still remain as to why such consistent experimental values were obtained.

Pa-1 also can be regarded as an extreme case of In-experiment but the measured value for a single rod in the position of 14-19 (or 22-17) is not known. However, assuming it to have the same reactivity worth with 14-18, the interaction factor becomes 0.791 from the data of B2, suggesting how strong is the self-shielding of the B_4C simulating control rods in this core.

We conducted the following supplementary experiments in relation to the uncertainty of the experimentally obtained values. In view of the fact that the safety control rod has a reactivity worth higher than that of ordinary fuel drawers and this is suspected to have some

---

* In the case of 4B experiments the interaction factor defined in the same way as above becomes 1.009 and the additivity is maintained within the experimental error.

** Refer to 3.1.2.

effect on the reactivity worth of B_4C simulating control rods around the core, we obtained the reactivity worth by the critical method by replacing the central 1-pin in the sodium channel of 16-22 with B_4C pin. When it was inserted on the fixed and on the movable side, the obtained values agreed with each other within the range of experimental errors. This fact does not immediately means that there is no influence of the FCA control rods. However, it is already known that there is no interaction with the fuel drawers around the control rods in V-2 assembly and therefore we concluded that there was no local effect on the worth of B_4C control rod located in the vicinity of the FCA control rods. Next, we removed the three pins at the middle stage of the seven pins of the sodium channel and measured their reactivity worths because it was impossible to make a quantitative investigation of the chemical composition of the Calandria when it was manufactured. This reactivity worth was 0.19 ρ o in the position of F16-22 and this quantity is negligible as compared with the reactivity worth of the B_4C simulating control rod.

In the preface, we said that we made measurements by the critical method and the pulsed neutron method at the same time. Although the experimental values obtained in these measurements are not definite at the present stage, the experimental values obtained by the neutron source multiplication method are approximately equal to those obtained by the critical method and several percents to 10 percents larger than those obtained by the pulsed neutron method.

4. Calculated values of reactivity worths of B_4C simulating control rods

4.1 Process of calculations

4.1.1 Outline

As for the analytical calculations for the B_4C simulating rod experiments on V-3 assembly, it is inevitable to employ mainly the two-dimensional calculation due to the nature of the problem. There are still so much performance restrictions to the computer for making two-dimensional calculations that it is impossible to use the sufficient numbers of energy groups and space meshes in solving the two-dimensional equations. This being so, it is necessary to determine a suitable group collapsing and space mesh interval and also to know in advance the resultant deviations from the standard calculations.

We made the survey calculations of the above-stated effects all by one-dimensional calculation method and applied thus obtained results to the two-dimensional calculations. The one-dimensional diffusion code EXPANDA-4[8] was used for the survey calculations. The flow of the survey calculations and the worth calculations are schematically presented in Fig. 8. As for the group constants, we used the 25-group JAERI-FAST Version II[7] which has been collapsed from 70 groups. We used the calculated values obtained by the 25-group set as a standard for checking the group collapsing effect.

The configuration of the system and the atomic number densities are given in Table 1.

Unlike ordinary fuel drawers, the safety and control rods of V-3 assembly are not loaded with Pu. They are loaded with U alone and are spiked as a whole. However, these effects were not considered in constructing a model of the calculation system.

The results of the various steps in the flow of calculation in Fig. 8 will be discussed in Appendix (A4). Here we will explain the flow of calculation and the overall results.

4.1.2 Collapsing of group constants

The system we used for checking the group collapsing effect was 35.4 cm in radius and is fitted with 28.5 cm thick natural uranium blanket in the radial direction. The six sodium channels around the

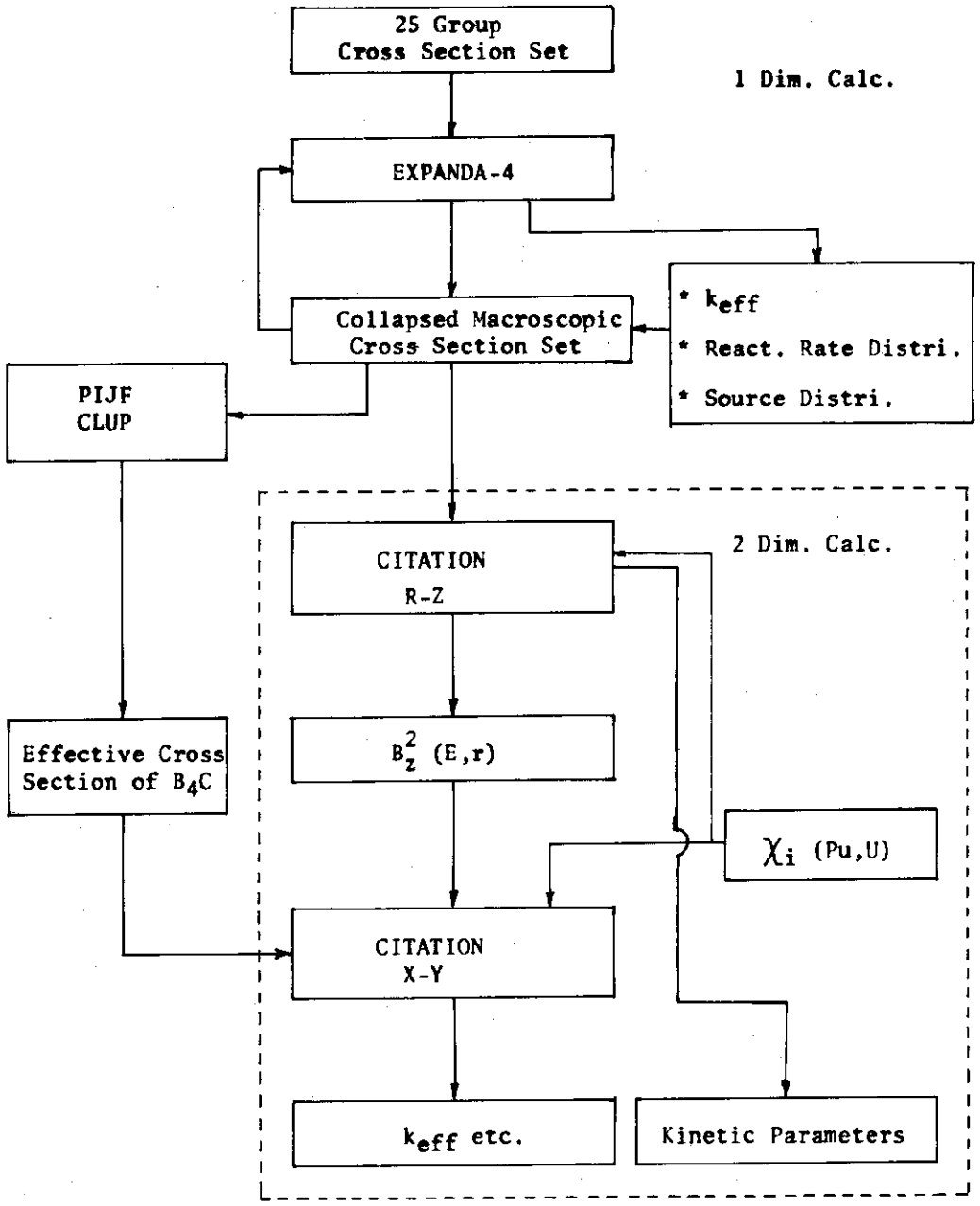

Fig. 8 Flow chart of calculations

core are mixed homogeneously with the core material and arranged in a circular ring. We made calculations, using various collapsed group NG in the case in which a simulating control rod is inserted in the center of the system (BC1) and also in the case in which the system is clean with no such rod is inserted (CL1) to observe the deviation of the reactivity worth of B_4C simulating control rod defined by $\delta\rho_{NG}=(K_{NG}^{CL1}-K_{NG}^{BC1})/K_{NG}^{CL1}\cdot K_{NG}^{BC1}$ from the standard value of the 25-group set. As a result we found that $\delta\rho_{NG}$ had a very good parallelism in CL1 and BC1 and $\delta\rho_{NG}$ itself showed little change if the group number was changed. The deviation of $\delta\rho_{NG}$ from $\delta\rho_{25}$ was only about 0.53% even at NG = 4, that is, the largest of the NGs we had calculated. (Refer to Appendix (A4)) From this, it may be concluded that both the k_{eff} of the clean system and the k_{eff} of a system having a local absorbing region show an almost parallel behavior for the group collapsing. The neutron flux distribution can be considered to represent the differential quantity of the whole system while k_{eff} represents the integral quantity of the whole system. The dependence of this quantity on the collapsed group number NG must be considered in determining the collapsed group number. For this reason, we calculated the B_4C reactivity distribution for each NG to observe the deviation from the distribution for NG = 25. (Refer to Appendix (A4))

Thus we finally determined NG = 8. As for the deviation of collapsed groups, the groups up to the 14th were grouped in two and the 15th and the following groups were made in one group. As a result the 8-group calculation is presumed to estimate the reactivity worth of B_4C simulating control rod about 0.13% larger than the 25-group calculation.

4.1.3 Buffer region

Since the neutron spectrum is considered to change in the region near the highly absorbing B_4C simulating control rod and in the region near the boundary of the core blanket, these regions were specially made the buffer regions and their spectra were used to make the collapsed cross section for each region. (Refer to Appendix (A5.1)) The 8-group cross sections calculated in each region are given in Table 10-1 through Table 10-4. The table is divided into blocks for the respective regions. The figures in the row represent

the region No., group No., D, Σ a, and $\nu\Sigma$f from left and those in the second and third rows represent $\Sigma_s^{i\to j}$ $(i<j)$. The fourth row is the same with the top row and the following rows are also the same as the second and third rows. The region No. matches the region No. in Fig. 11.

4.1.4 Fission spectrum

As for the fission spectrum χ i, we used the average value obtained with the number of the neutrons produced by the actual fission on Pu and U as the weights. (Appendix A5.2) The values of χi of the eight groups which were used are given in Table 11.

Table 11 χ i values for 8-group calculation

i	1	2	3	4	5	6	7	8
i	0.1090	0.4490	0.3437	0.0862	0.0113	0.0008	0.0	0.0

4.1.5 B_4C 7-pin cluster

The B_4C simulating control rod has seven B_4C pins of 0.55 cm in radius arranged in a cluster in sodium as illustrated in Fig. 6-(a). The macroscopic cross section of this section was obtained by use of the calculation code PIJF, CLUP(9) of the collison probability method. For the calculation, we used a model as illustrated in Fig. 6-(b) and the 8 groups as determined in 4.1.2. The calculated neutron flux distribution is shown in Fig. 9, in which the smooth curve represents the neutron flux distribution when B_4C and Na are mixed homogeneously and the ordinary diffusion approximation method was used while the stepped graph shows the neutron flux distribution obtained by the collision probability method. There are double lines in the second B_4C region as viewed from the rod center. The upper line represents the distribution between the B_4C pins (distribution on OA in Fig. 9) and the lower line represents the distribution passing through the B_4C pin (distribution on OB in Fig. 9). The effective cross section of the B_4C region was obtained by thus obtained neutron flux and the results are given in Table 12, in which are also given the group constants collapsed by the spectrum obtained by the diffusion approximation method with B_4C and Na being homogeneously mixed. Comparing these results, paying attention to Σ a, it is found that the values obtained by collison probability

method are about 5% to 11% smaller than those which were obtained by the diffusion approximation method in the 3rd and 4th groups near the neutron flux peak. This tendency is further pronounced as the group number increases. This fact shows that the effective cross section obtained by the collision probability method gives the B_4C simulating control rod reactivity worth about 7.0%[note)] lower than that which is obtained by the homogeneous diffusion approximation calculation.

We had only three 7-pin type B_4C simulating control rods and consequently we had use the one-rod type rods when it was necessary to make an experimental system in which four or more B_4C simulating control rods were to be inserted. However, in our calculations, we regarded all the rods as the 7-pin type and did not calculate the effective cross sections of the one-rod type rods but used the effective cross sections calculated in this paragraph. The conversion of the reactivity worths of the 7-pin type and one-rod type B_4C simulating control rods was made experimentally. (Refer to 3.3.1)

Note) This comparison of reactivity worths of B_4C simulating control rods was made when the 7-pin type rods were inserted in the core center. The results were as given below.

	Homo k_{eff}	Hetero k_{eff}
NC1	0.985171	0.985171
BC3	0.958719	0.960580
	0.0280 Δk/k	0.0260 Δk/k

Table 10-1 8-group macroscopic cross section

```
    1      1 3.36023      1.01503E-02 2.54146E-02
                          3.24241E-02 2.18272E-02 5.46212E-03 5.52958E-04 1.81434E-05
4.53585E-09 0.0
    1      2 2.67121      7.47535E-03 1.98222E-02
                          3.00670E-02 6.59186E-03 1.33485E-03 5.78393E-05
4.25120E-06
    1      3 1.80822      4.86016E-03 1.01536E-02
                                      2.10026E-02 5.05709E-04 1.49936E-05
2.25835E-07
    1      4 1.35426      5.63597E-03 1.03458E-02
                                                  1.13380E-02 1.22429E-05
4.26803E-07 3.15840E-07
    1      5 1.10490      8.81232E-03 1.28882E-02
                                                              6.32260E-03
9.64398E-07 9.16406E-09
    1      6 0.955381     1.38569E-02 1.70698E-02
8.93796E-03 6.17501E-07
    1      7 0.664707     2.63331E-02 3.07998E-02
                          8.61498E-03
    1      8 0.877168     4.64007E-02 6.40297E-02

    2      1 3.36131      1.01667E-02 2.54504E-02
                          3.24072E-02 2.18161E-02 5.45477E-03 5.52029E-04 1.81057E-05
4.52264E-09
    2      2 2.67178      7.47617E-03 1.98267E-02
                          3.00387E-02 6.59552E-03 1.33345E-03 5.77959E-05
4.24382E-06
    2      3 1.79513      4.84867E-03 1.00893E-02
                                      2.19278E-02 4.71264E-04 1.38564E-05
2.20456E-07
    2      4 1.35442      5.63476E-03 1.03445E-02
                                                  1.13122E-02 1.22458E-05
4.27502E-07 3.16491E-07
    2      5 1.10576      8.78903E-03 1.28727E-02
                                                              6.18984E-03
9.77265E-07 9.29847E-09
    2      6 0.961641     1.37627E-02 1.69948E-02
8.34069E-03 5.75925E-07
    2      7 0.659317     2.61985E-02 3.06176E-02
                          8.29917E-03
    2      8 0.876818     4.64826E-02 6.41539E-02

    3      1 1.94264      2.76200E-02 8.46362E-02
                          3.32717E-02 6.21688E-02 1.97646E-02 1.96740E-03 8.82495E-05
3.05773E-08
    3      2 1.57999      2.19550E-02 5.42515E-02
                          6.53560E-02 2.91380E-02 7.41204E-03 3.15423E-04
7.90764E-06
    3      3 1.23055      6.32709E-03 1.93501E-03
                                      2.19323E-02 1.23980E-03 2.20446E-05
1.14909E-07
    3      4 0.85241      6.91047E-03 1.02567E-03
                                                  1.08560E-02 1.03608E-05
8.62339E-08 6.48126E-08
    3      5 0.618118     1.46982E-02 1.44654E-03
                                                              3.01880E-03
3.06781E-06 1.95546E-09
    3      6 0.603525     2.30966E-02 2.02106E-03
1.40652E-03
    3      7 0.750486     2.76054E-02 3.03815E-03
                          2.04288E-03
    3      8 0.725269     2.58187E-02 7.83627E-03

    4      1 1.94441      2.77686E-02 8.52415E-02
                          3.36205E-02 6.20173E-02 1.96288E-02 1.95308E-03 8.75495E-05
3.02152E-08
    4      2 1.58262      2.19822E-02 5.44002E-02
                          6.53380E-02 2.91530E-02 7.34675E-03 3.13116E-04
7.79413E-06
    4      3 1.20634      6.22022E-03 1.56279E-03
                                      2.06539E-02 9.61078E-04 1.42078E-05
1.07386E-07
    4      4 0.853087     6.90250E-03 1.02490E-03
                                                  1.07640E-02 1.02920E-05
8.67364E-08 6.52772E-08
    4      5 0.619454     1.45550E-02 1.44152E-03
                                                              2.89737E-03
3.12967E-06 2.00439E-09
    4      6 0.604328     2.27808E-02 2.00730E-03
1.09315E-03
    4      7 0.739289     2.77677E-02 2.97830E-03
                          1.65456E-03
    4      8 0.723023     2.58392E-02 7.87113E-03
```

Table 10-2 8-group macroscopic cross section

```
    5      1 5.42070      1.03970E-03 0.0
             2.52702E-02 1.24660E-02 2.35668E-03 2.01388E-04 3.98665E-06
    5      2 4.83656      1.79811E-04 0.0
                           1.55093E-02 1.71501E-03 2.22782E-04 1.10185E-05
4.20119E-06
    5      3 3.51503      1.02022E-04 0.0
                                       7.51959E-03 1.53762E-04 8.28999E-06
2.81485E-07
    5      4 2.85711      1.55988E-04 0.0
                                                   5.73844E-03
    5      5 2.21079      4.22399E-04 0.0
                                                               4.03932E-03
    5      6 1.40563      5.46699E-04 0.0
1.00918E-02
    5      7 0.776714     1.87585E-03 0.0
                7.14890E-03
    5      8 1.32667      5.27842E-04 0.0
```

```
    6      1 3.36007      1.01478E-02 2.54092E-02
             3.24266E-02 2.18289E-02 5.46322E-03 5.53097E-04 1.81490E-05
4.53783E-09
    6      2 2.67033      7.47409E-03 1.98155E-02
                           3.01099E-02 6.58632E-03 1.33697E-03 5.79051E-05
4.26237E-06
    6      3 1.80848      4.86040E-03 1.01550E-02
                                       2.09838E-02 5.06409E-04 1.50167E-05
2.25944E-07
    6      4 1.35397      5.63806E-03 1.03479E-02
                                                   1.13822E-02 1.22379E-05
4.29405E-07 3.14724E-07
    6      5 1.10469      8.81806E-03 1.28921E-02
                                                               6.35535E-03
9.61225E-07 9.13090E-09
    6      6 0.954847     1.38649E-02 1.70762E-02
8.98895E-03 6.21050E-07
    6      7 0.671609     2.65055E-02 3.10331E-02
                9.01945E-03
    6      8 0.875718     4.67661E-02 6.45660E-02
```

```
    8      1 3.57980      0.93723E-02 0.0
             0.36566E-01 0.15655E-01 0.26698E-02 0.23513E-03 0.45025E-05
    8      2 2.9725       0.63836E-02 0.0
                           2.44548E-02 0.17605E-02 0.22385E-03 1.09054E-05
4.8365 E-06
    8      3 1.98915      8.6394 E-03 0.0
                                       2.18974E-02 1.81178E-04 1.00388E-05
3.76385E-07
    8      4 1.49140      2.57412E-02 0.0
                                                   1.52338E-02 4.39564E-06
0.59535E-06 0.66565E-07
    8      5 1.18149      5.47088E-02 0.0
                                                               8.32717E-03
    8      6 0.76541      0.99041E-01 0.0
1.26952E-02
    8      7 0.37288      0.15676     0.0
                1.25174E-02
    8      8 0.57259      0.22882     0.0
```

```
    9      1 3.36020      1.01498E-02 2.54136E-02
             3.24245E-02 2.18275E-02 5.46233E-03 5.52983E-04 1.81444E-05
4.53621E-09
    9      2 2.67005      7.47369E-03 1.98133E-02
                           3.01236E-02 6.58454E-03 1.33765E-03 5.76262E-05
4.26596E-06
    9      3 1.81058      4.86223E-03 1.01652E-02
                                       2.08359E-02 5.11914E-04 1.51985E-05
2.26804E-07
    9      4 1.35477      5.63215E-03 1.03418E-02
                                                   1.12570E-02 1.22520E-05
4.28996E-07 3.17882E-07
    9      5 1.10674      8.76264E-03 1.28551E-02
                                                               6.03946E-03
9.91840E-07 9.45072E-09
    9      6 0.960908     1.37738E-02 1.70035E-02
8.41060E-03 5.80791E-07
    9      7 0.655760     2.61097E-02 3.04973E-02
                8.09070E-03
    9      8 0.879072     4.59494E-02 6.33600E-02
```

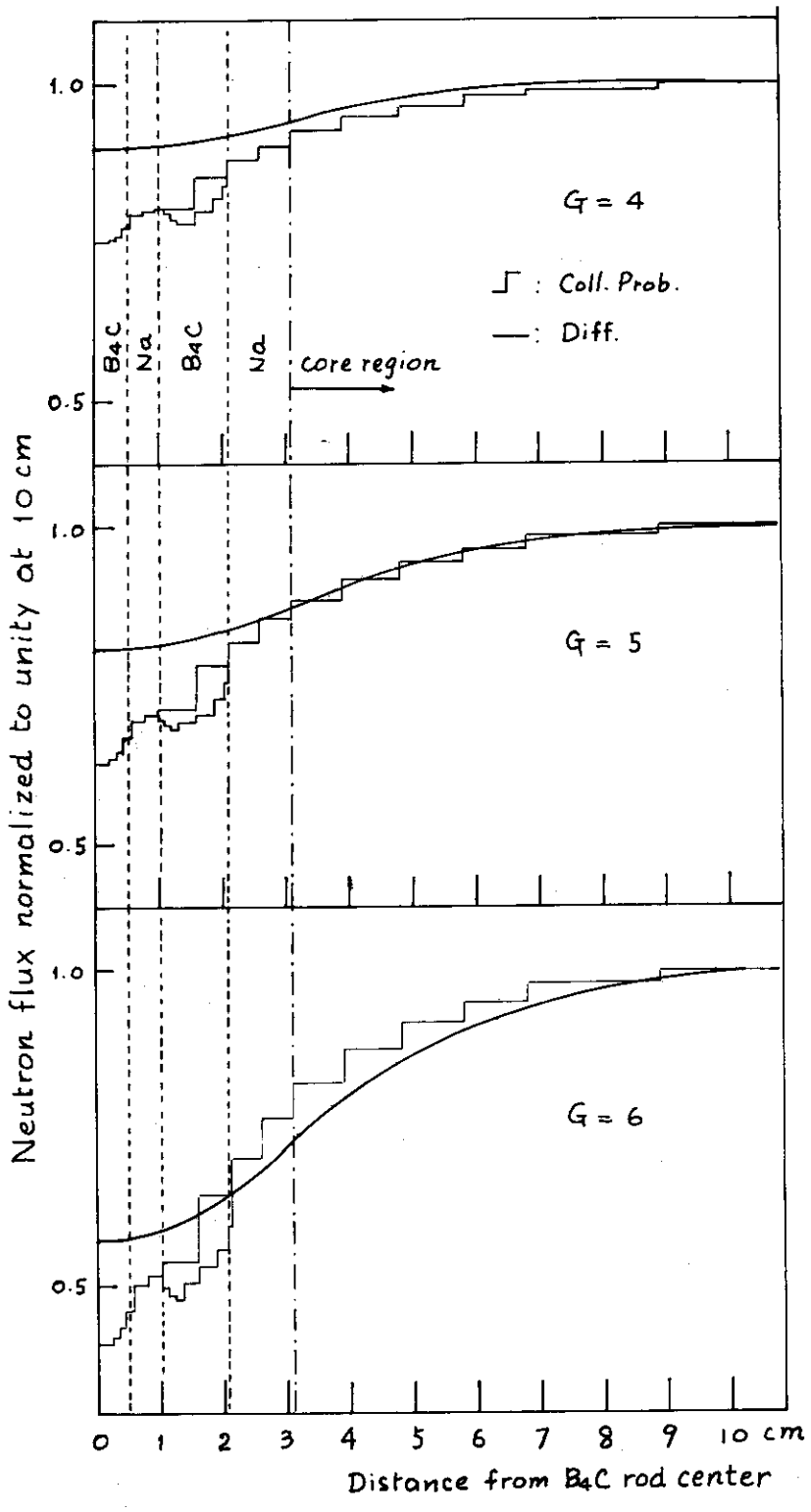

Fig. 9 Neutron flux distribution in and around the B_4C rod

Table 12 Comparison between collapsed data from diffusion calculation and those from collision probability calculation

	Diffusion(1)		Collision Probability(2)	
G	D	SIGMA A	D	SIGMA A
1	3.5103	9.5535 (-3)	3.5798	9.3723 (-3)
2	2.9219	6.5683 (-3)	2.9725	6.3836 (-3)
3	2.0170	9.0770 (-3)	1.9892	8.6394 (-3)
4	1.4052	2.9058 (-2)	1.4914	2.5741 (-2)
5	1.1468	6.0960 (-2)	1.1815	5.4709 (-2)
6	0.7550	1.2500 (-1)	0.7654	9.9041 (-2)
7	0.3640	2.8423 (-1)	0.3729	1.5676 (-1)
8	0.3567	5.6974 (-1)	0.5726	2.2882 (-1)

(1) EXPANDA-4 JAERI-FAST Version-2

(2) PIJF, CLUP JAERI-FAST Version-2

4.1.6 The effects of space meshes

A total of 84 space meshes are to be used in the standard calculation of the one-dimensional survey, that is, 8 meshes for the B_4C region, 46 meshes for the core region and 20 meshes for the blanket region. However, we reduce the number of the meshes to about 50 due to the restrictions of the two-dimensional calculation. (Appendix A5.3) If the number of the meshes is reduced in an appropriate method, the effect is so small that the reactivity worth of B_4C simulating control is estimated only 0.03% lower than the standard calculated value. As a result, it is presumed that the reactivity worth of B_4C simulating control is estimated about 0.1% higher than the standard value due to the effects of the group collapsing and the number of the space meshes. This will be discussed in detail in Chapter 5.

4.1.7 Transverse buckling calculation

It is necessary for the two-dimensional calculation to be made by the X-Y coordinates so that the B_4C simulating control rod positions in the core may be faithfully reproduced. Therefore, the two-dimensional R-Z calculation must be made beforehand to determine the transverse buckling in the Z direction of each region. This calculation was made by use of the diffusion calculation code CITATION.[10)]

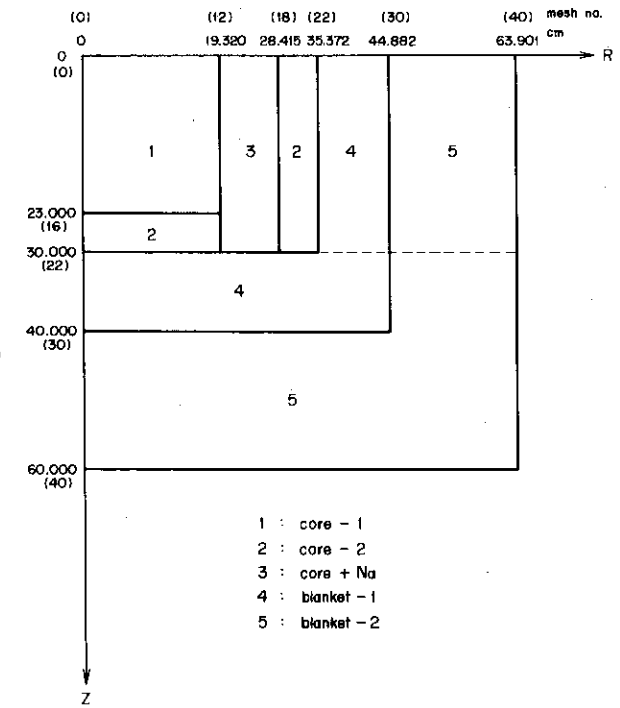

Fig. 10 Clean core system for R-Z calculation

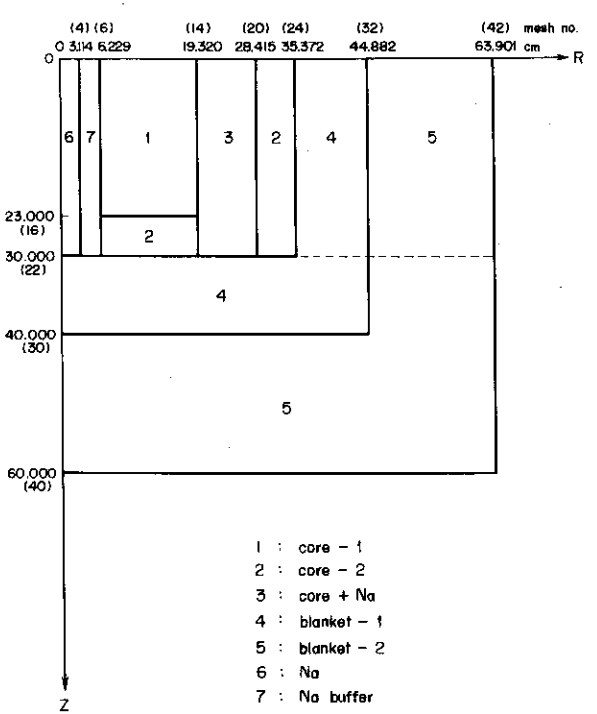

Fig. 11 Core system containing a Na channel at the center for R-Z calculation

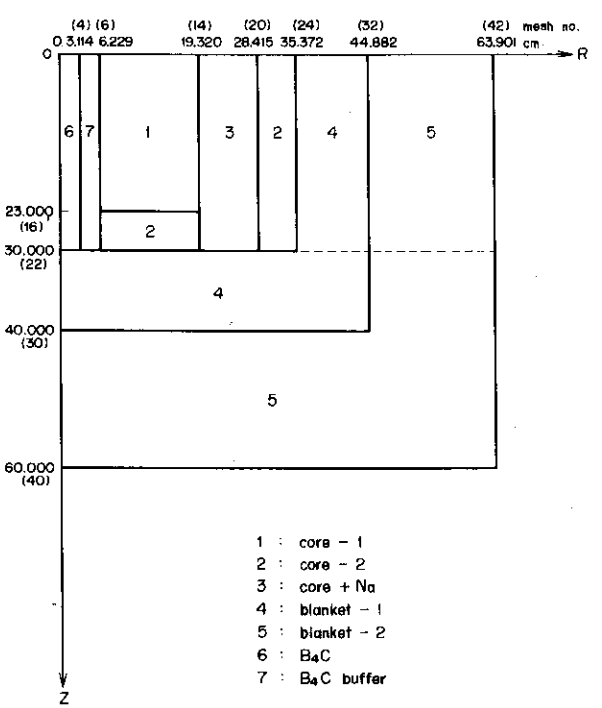

Fig. 12 Core system containing a B_4C rod at the center for R-Z calculation

The calculation systems are illustrated in Figs. 10, 11 and 12. Fig. 10 shows a clean core system (in which the sodium and core material mixed regions are arranged in a ring in the peripheral area), Fig. 11 shows a core system containing a sodium channel in the center, and Fig. 12 shows a core system containing a B_4C simulating control rod replacing the sodium channel. These systems were calculated by the R-Z coordinates and B_z^2 of each energy group and region was obtained, assuming that the number of neutron leaking outward in the Z direction from the extended plane of the end surface of the core is equal to $D_i B_z^2 \bar{\phi} V$. (Refer to Appendix 6) Here it must be noted that B_z^2 of sodium channel and B_4C simulating control region can be obtained only in the core center. In the actual two-dimensional X-Y calculation, B_z^2 that is obtained in the core center is used at the real position and it does not seem to bring about any large error within the range in which the equilibrium spectrum is realized. Table 13 gives the transverse bucklings dependent on the regions and energy groups. There are some limits encountered in using thus obtained transverse bucklings in the two-dimensional calculation. That is to say that the number of neutrons leaking out of the core in the Z direction (when Z-direction blanket is provided) is estimated in the form of $DB_z^2 \phi$ but no consideration is given to the contribution of the Z-direction blanket to the reactivity and other effects. On the other hand, however, when the same system is compared with the results of calculation by the two-dimensional RZ coordinates, other effects seem to be negligible. (Refer to 4.2.2)

4.1.8 Two-dimensional XY calculation

Preparations have now been made for the two-dimensional XY calculation, which was made by use of the CITATION code as the R-Z calculation. The whole X-Y calculation system is illustrated in Fig. 13. The regions enclosed by dotted lines are the buffer regions for the inner regions enclosed with the solid lines.

Calculations were made for the following cases. The characters Q, H and F at the end of the symbols means that the calculations were made with such conditions as 1/4 symmetry, 1/2 symmetry and nonsymmetry, respectively.

(1) CQ: Clean system with six sodium channels in the periphery.
(2) NCQ: System with a sodium channel in the center of the CQ

system (in the position of 18-18).

(3) BCQ: System with B_4C simulating control rod in place of sodium channel in the NCQ system.

(4) 2BQ: System with B_4C simulating control rods in the positions of 14-18 and 22-18.

(5) 4BQ: System with B_4C simulating control rods in the positions of 16-14, 16-22, 20-14 and 20-22.

(6) 6BQ: System with B_4C simulating control rods in the positions of 14-18, 16-14, 16-22, 20-14, 20-22 and 22-18.

(7) TC2Q: The core system for the radial traverse in which the sodium channels in the positions of 14-18 and 22-18 are moved to 15-18 and 21-18, respectively.

(8) TR2Q: System with B_4C simulating control rods inserted in the sodium channels which were moved in the TC2Q system.

(9) TC3Q: System with the sodium channels moved further inward (16-18 and 20-18) than in the TC2Q system.

(10) TR3Q: System with B_4C simulating control rods inserted in the positions of the sodium channels moved in the TC3Q system.

(11) CH: Clean system, calculated with 1/2 symmetry.

(12) 1BH: System with B_4C simulating control rod inserted in the position of 14-18.

(13) 5BH: System with B_4C simulating control rods inserted in the positions of 14-18, 16-22, 20-22, 20-14 and 16-14.

(14) CF: Clean system, calculated without using symmetry. (Reference of F series)

(15) B2F: System with B_4C simulating control rod inserted in the position of 14-18.

(16) B1F: System with B_4C simulating control rod inserted in the position of 16-22.

(17) 1N1F: System with B_4C simulating control rods inserted in the positions of 14-18 and 20-22.

(18) 1N2F: System with B_4C simulating control rods inserted in the positions of 14-18 and 16-22.

(19) 1N3F: System with B_4C simulating control rods inserted in the positions of 16-22 and 20-22.

(20) 2BF: System with B_4C simulating control rods inserted in the positions of 14-18 and 22-18.

Table 13 Region-Grou-Dependent Bucklings

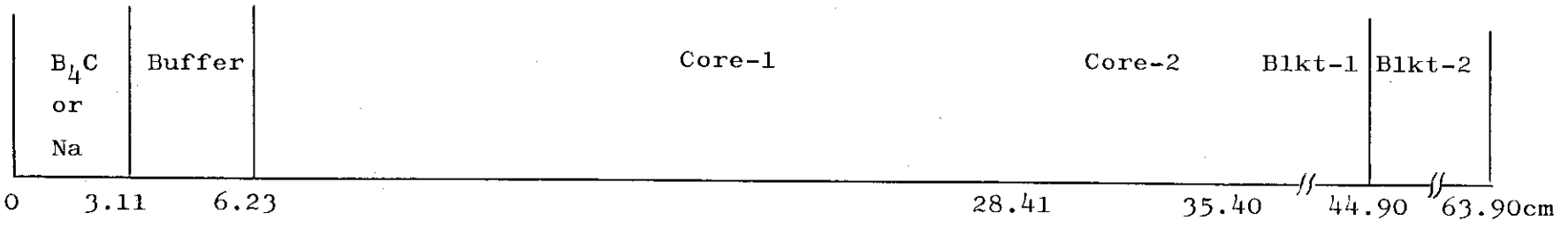

	B_4C	B_4C Buffer	Na	Na Buffer	Core-1	Core-2	Blanket-1	Blanket-2
1	1.6914(-3)	1.9298(-3)	1.3209(-3)	1.9643(-3)	1.9763(-3)	2.0100(-3)	2.0513(-3)	1.3077(-3)
2	1.7832(-3)	2.0122(-3)	1.3133(-3)	2.0510(-3)	2.0383(-3)	2.0914(-3)	2.0841(-3)	1.3245(-3)
3	8.6960(-4)	1.0710(-3)	7.2451(-4)	1.1407(-3)	1.1240(-3)	1.2316(-3)	1.4461(-3)	1.1829(-3)
4	4.1137(-4)	6.0773(-4)	4.9319(-4)	8.3037(-4)	8.3361(-4)	9.5771(-4)	1.2756(-3)	1.0963(-3)
5	5.8603(-5)	1.0822(-3)	5.0796(-4)	8.1381(-4)	7.9627(-4)	9.2345(-4)	1.2389(-3)	1.0489(-3)
6	3.6906(-5)	1.2680(-3)	1.1791(-3)	1.5208(-3)	1.4996(-3)	2.4164(-3)	1.4365(-3)	1.0547(-3)
7	-2.1160(-3)	2.5969(-3)	2.8185(-3)	2.7379(-3)	2.6939(-3)	2.7437(-3)	1.6748(-3)	1.1864(-3)
8	-1.0366(-3)	1.5736(-3)	1.7176(-3)	1.9373(-3)	1.8211(-3)	1.8760(-3)	1.6260(-3)	1.2497(-3)

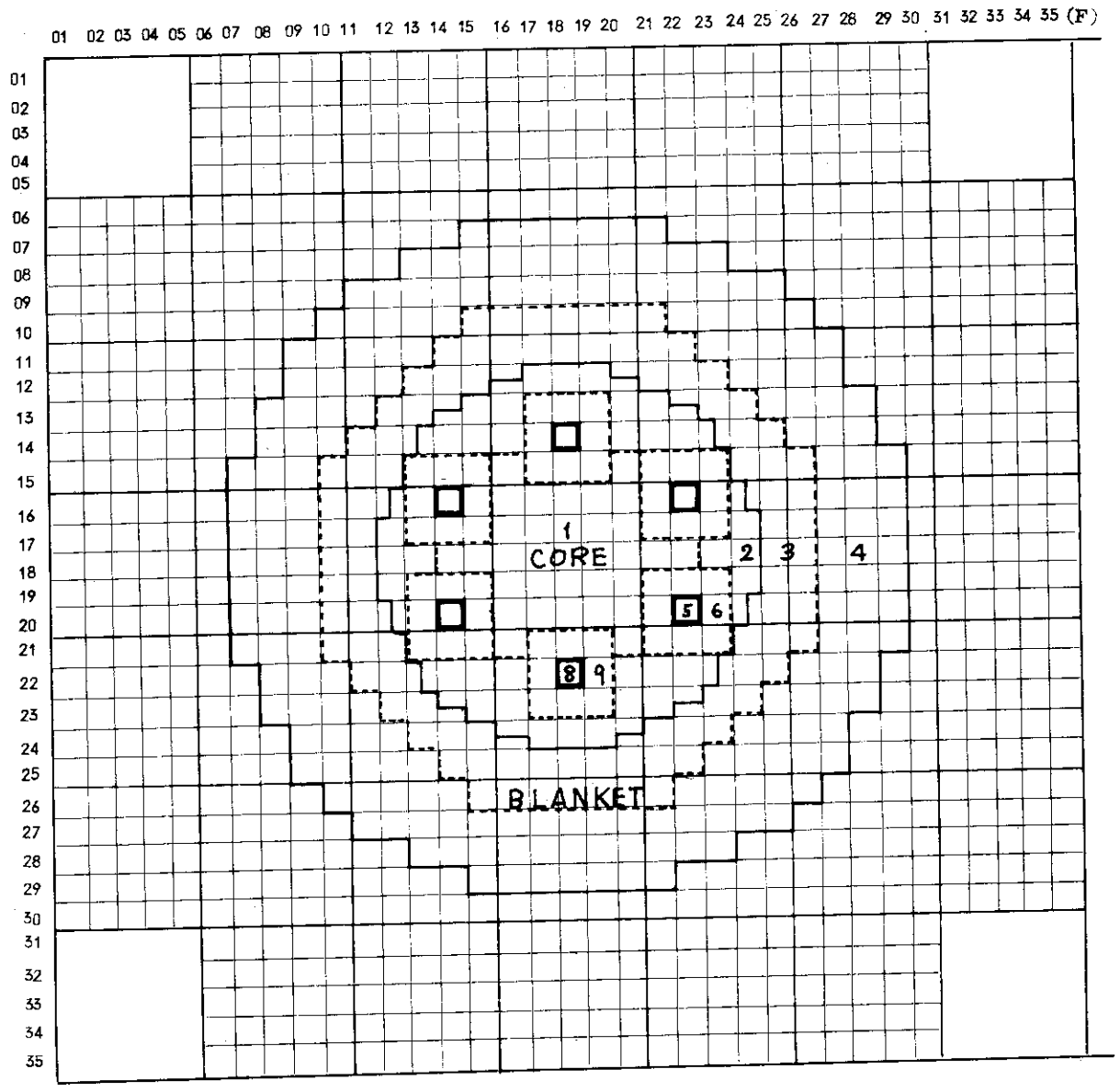

1. Core-1
2. Core-2
3. Blanket-1
4. Blanket-2
5. Na
6. Na-buffer
7. Dummy
8. B_4C+Na
9. B_4C+Na-buffer

Fig. 13 FCA assembly V-3 (Illustrated for calculation)

(21) PCF: Clean system with sodium channels added in the positions of 14-19 and 22-17 in the CF system, the standard system with a pair of B_4C simulating control rods.

(22) PA1F: System with B_4C simulating control rods inserted in the positions of 14-18 and 14-19.

(23) PA2F: System with B_4C simulating control rods inserted in the positions of 14-18, 14-19, 22-18 and 22-17.

The systems corresponding to the above symbols are illustrated in Fig. 7-1 and Fig. 7-2.

It is necessary to make the following corrections to the calculated values and further details will be discussed in 4.2 and 4.4.

(1) Calculation corrections by the transport theory

(2) Critical experiment corrections

(3) Corrections required by the construction of the B_4C simulating rod

4.2 Criticality

4.2.1 Outline

The main object of the analysis of this experiment is to obtain the eigenvalue of the sub-critical system with a single or two or more B_4C simulating control rods inserted in the core and obtain the reactivity worth of the B_4C simulating control rod as a deviation from the eigenvalue of the standard system (clean critical system). It is important for the eigenvalue of the standard system itself to faithfully reproduce to experimental value so that the reactivity worth calculation may have a high degree of reliability. This being so, in this paragraph we will discuss how faithfully the experimental value is reproduced for the eigenvalue of the standard system which was obtained by the two-dimensional calculation method. Since the comparison is made of the eigenvalues, experimental corrections were applied to the calculated value in order to maintain the experimental value at the critical time as 1,000,000.

4.2.2 Comparison with the experimental results

The two dimensional eigenvalue calculations were made by use of R-Z coordinates or X-Y coordinates. Different corrections must be applied to the calculated values obtained by the two different coordinates. Such corrections are given in Table 14. The corrected

Table 14 Several correction factors applied to the calculated eigenvalues

Coordinate / k_{eff} (Un-Corrected) / Corrections	RZ	XY					
		CQ	CH	CF	TC2Q	TC3Q	PCF
	0.9956354	0.9926268	0.9929819	0.9936019	0.9900035	0.9875225	0.9853880
Excess reactivity	-0.003027	-0.003027	-0.003027	-0.003027	-0.00028796	+0.001431	+0.006975
Effect of spiked S/R & C/R	+0.007054	+0.007054	+0.007054	+0.007054	+0.007054	+0.007054	+0.007054
Gap effect	-0.002654	-0.002654	-0.002654	-0.002654	-0.002654	-0.002654	-0.002654
Core boundary effect	-0.000630						
Heterogeneity effect	+0.003344	+0.003344	+0.003344	+0.003344	+0.003344	+0.003344	+0.003344
Total $\delta k/k$	+0.004087	+0.004717	+0.004717	+0.004717	+0.007456	+0.009175	+0.014719
k_{eff} (corrected)	0.999703	0.997296	0.997655	0.998281	0.997366	0.996552	0.999890

eigenvalues given in the bottom row in the table are the quantities to be directly compared with the experimental value 1,000,000 and they are well in agreement with one another with differences amounting only to 0.3% at most. In this case, however, the S_N correction is not made to the calculated values. The correction items in Table 14 are those which were discussed in 2.4. All other cases than PCF by the X-Y calculation give eigenvalues slightly smaller than the values obtained by the RZ calculation method. This is presumably due to the way the Z-direction blanket was treated in the X-Y calculation. As for the values obtained by the X-Y calculation, the Q series given relatively low eigenvalues and the H and F series give higher values in that order. This is presumably due to the influence of the space mesh size (the mesh interval sizes are smaller in the order of Q, H and F) used in the calculations.

4.3 Kinetic parameters calculation

The calculation of kinetic parameters is important in determining the experimental standard reactivity worth ρ_0 and have an effect on the whole experimental values. As for the group constants, we used JAERI-FAST version II[7] which was used for the calculation of the aforesaid eigenvalues and the collapsed 8-group cross section in the two-dimensional calculation. As for β_i^m, Sandmeier[11] was used as the source data for U-238, Pu-239, Pu-240 and Pu-241 and Keepin[3] for U-235. The delayed fission neutron spectrum χ_d is shown in Table 15.

Table 15 Delayed fission neutron spectrum χ_d

group \ isotope	Pu-239	Pu-240	Pu-241	U-235	U-238
1	0.	0.	0.	0.	0.
2	0.	0.	0.	0.	0.
3	0.4309	0.4350	0.4417	0.4292	0.4404
4	0.5691	0.5650	0.5583	0.5708	0.5596
5	0.	0.	0.	0.	0.
6	0.	0.	0.	0.	0.
7	0.	0.	0.	0.	0.
8	0.	0.	0.	0.	0.

When requires special attention with regard to the calculation of β_{eff} is the degree of contribution made by U-238 fission neutrons. This means that the fission rate of U-238 must be calculated faithful to the experimental system. For this purpose, the FCA control and safety rods were considered faithfully. (These rods contains no Pu but a large amount of 20% enriched uranium). It is also necessary with regard to the blanket to obtain a correct value of the fission rate. This required at least two-dimensional calculation. The two-dimensional calculation was made on the R-Z system by use of the CITATION code and the sodium channels were diluted homogeneous in a ring shape.

The calculated delayed fission neutron fraction β_{eff} was 0.548% and the lifetime of the prompt neutrons lp was $1.86_2 \times 10^{-7}$ S. For the sake of comparison,[note)] we considered a model calculation system and made the 25-goup one-dimensional calculation on the system by use of the ARGO code.[12)] A shape factor of 0.93 was used in the conversion to a spherical system and the critical adjustment was made by the radius of the central region. Thus obtained results showed no noticeable differences on the clean system as seen from Appendix (A7).

The standard reactivity worth ρ_0 which was obtained by the in hour equation $\rho = \frac{\ell}{T} + \sum_{i,m} \frac{\beta^m_{eff}}{1+\lambda^m_i T}$ for T = 144.87s was

$$\rho_0 = 0.0355_5 \ \% \ \delta k/k \ \pm 0.00029\% \ \delta k/k$$

λ^m_i and β^m_{effi} we used are given in Table 16 and Table 17. The values of β^m_{effi} were obtained by the two-dimensional calculation.

Table 16 Values of λ^m_i

(sec^{-1})

group / isotope	1	2	3	4	5	6
Pu-239	0.0128	0.0301	0.1238	0.3254	1.122	2.697
Pu-240	0.0129	0.0313	0.1349	0.3332	1.356	4.030
Pu-241	0.0128	0.0299	0.1238	0.3519	1.612	4.621
U -235	0.0127	0.0317	0.115	0.311	1.40	3.87
U -238	0.0132	0.0321	0.139	0.358	1.41	4.02

Note) The group collapsing effect is taken into consideration.

Table 17 Values of β^{m}_{effi} by 2-dimensional calculation

(%)

group / isotope	1	2	3	4	5	6
Pu-239	0.002532	0.021942	0.015552	0.023991	0.006269	0.003255
Pu-240	0.000061	0.000659	0.000449	0.000874	0.000330	0.000066
Pu-241	0.000028	0.000656	0.000495	0.001114	0.000521	0.000045
U -235	0.011019	0.061742	0.054504	0.118010	0.037090	0.007540
U -238	0.002332	0.024587	0.029068	0.069636	0.040385	0.013466

4.4 Calculation of reactivity worths

4.4.1 Definition of reactivity worth

The reactivity worth of B_4C simulating control rod is defined by the following equation with a core containing Na channels in the prescribed positions.

$$\delta\rho = \frac{1-K^{ref}_{eff}}{K^{ref}_{eff}} - \frac{1-K^{B}_{eff}}{K^{B}_{eff}} = -\frac{K^{ref}_{eff}-K^{B}_{eff}}{K^{ref}_{eff}\cdot K^{B}_{eff}}$$

where k^{ref}_{eff} and k^{B}_{eff} are the effective multiplication factors for the standard system and the system containing B_4C simulating control rods, respectively.

4.4.2 Calculated values of reactivity worth

The effective multiplication factor for each core pattern and reactivity worths obtained from them are given in Table 18. The eigenvalues may be reliable up to somewhere around 2×10^{-5} from the condition of convergence at the time of numerical values calculation. Therefore, calculation accuracy of reactivity worth becomes $\pm 3 \times 10^{-3}$. Considerably different values of reactivity worth were obtained in the calculations of Q-, H- and F-. This is presumably due to the mesh interval effect. This will be studied further in 5.3.2.

4.4.3 Calculated values of interaction factor

The calculated value of f_{ij} defined in 3.3.3 are given in Table 19. Judging from the reliability of the calculated eigenvalues,

the interaction factors can be considered to be reliable up to $\pm 4 \times 10^{-3}$. There is only example for observing the mesh interval effect. Looking at the interaction factors for 14-18 and 22-18, it is found that they are very well in agreement in the combination of Q- and H- and in the combination of F- and F- while there are very large disparities in such combinations as Q- and F- or H- and F-. From this observation, a reliability for the calculated values of other interaction factors, that is, in the combination of F- and F- may be obtained. This will be discussed in futher detail in 5.3.2.

Table 19 Calculated interaction factors f_{ij}

Positions		Distance (cm)	Systems used for calc of f_{ij}	f_{ij}
i	j			
16-22	20-22	22.08	IN3F, B1F	0.975
14-18	16-22	24.69	IN2F, B1F, B2F	0.988
14-18	20-22	39.81	IN1F, B1F, B2F	1.030
14-18	22-18	44.16	1BF, 2BQ	1.049*
14-18	22-18	44.16	B2F, 2BF	1.047*
14-17	22-18	44.16	PA1F, PA2F	1.078
14-18	22-19			

*) Same f_{ij}'s were calculated on two diffent systems, difference of which is negligibly small.

Table 18 Calculated k_{eff} and reactivity worth

No.	System	k_{eff}	$\delta\rho$ % δ k/k	Remarks
	CRZ	0.9956354		Clean R-Z Calc.
	NCRZ	0.9882827	0.747	Na at center R-Z Calc.
	BC3RZ	0.9616873	2.798	B_4C at center R-Z Calc.
(1)	CQ	0.9926268		Ref. of (2),(3),(4),(5),(6)
(2)	NCQ	0.9851818	0.761	
(3)	BCQ	0.9605820	2.599	
(4)	2BQ	0.9658524	2.793	=TR1Q
(5)	4BQ	0.9487175	4.663	
(6)	6BQ	0.9222431	7.688	
(7)	TR2Q	0.9900035		Ref. of (8)
(8)	TC2Q	0.9543033	3.779	
(9)	TC3Q	0.9875125		Ref. of (10)
(10)	TR3Q	0.9453028	4.522	
(11)	CH	0.9929819		Ref. of (12), (13)
(12)	1BH	0.9800321	1.331	
(13)	5BH	0.9369129	6.027	
(14)	CF	0.9936019		Ref. of (15)~(20)
(15)	B2F	0.9809287	1.300	
(16)	B1F	0.9830375	1.082	
(17)	IN1F	0.9699588	2.453	
(18)	IN2F	0.9705870	2.354	
(19)	IN3F	0.9732115	2.109	
(20)	2BF	0.9674302	2.723	=TR1F
(21)	PCF	0.9853880		Ref. of (22), (23)
(22)	PA1F	0.9647041	2.176	
(23)	PA2F	0.9418438	4.692	

5. A study of the ratio of calculated to experimental values (C/E)

5.1 Outline

The comparison of the ratios of calculated to experimental values (C/E) is made for various purposes.[note)] Since the experimental values obtained by the neutron multiplication method have problems about their reliability especially due to the possible inclusion of systematic errors, the purpose of the comparison is laid in the consistency of the C/E. When the C/E are consistently deviated from 1.0 for all items or when they have a certain definite tendency, some of the causes for such tendencies will be found out. When the C/E values are distributed around 1.0, the experimental and calculated values cannot be considered to be accurate solely for this reason. In this case, to find out why the values have come into agreement will be a complicated operation, requiring comparisons with the results of other experiments and calculations.

The comparison of the C/E values is made as follows. First, the C/E values are compared by using the previously obtained experimental and calculated values. Actually, these values are not to be compared directly. In any experiments and calculations, however, the raw data are valuable things because they are the starting point to which we must always return when we are encountered with some inconsistencies. The correction of raw data is always based on a phypothetical principle and it is the additivity of the reactivity and reactive worth in this paper. We call the C/E values the "primary comparison" (C/E raw data) and made a study of these data to find out systematic phenomena. On the other hand, the C/E values which have been corrected by consistent corrective values are called the "secondary comparison" (C/E corrected) in this paper. The experimental and calculated values were so corrected that they become the values which can be compared with one another.

5.2 Primary comparison (C/E raw material)

5.2.1 Comparison of B_4C simulating control rod reactivity worths

The uncorrected C/E values of the so far obtained experimental values (Table 8) and calculated values (Table 18) are given in

Note) Refer to Chapter 1.

Table 20. As for the calculated values, the C/E values become smaller in the order of Q, H, F. In the calculation on the same system, the calculated values obtained in Tr-1 experiment, for instance, are different between 2BQ and 2BF. The values are smaller in F calculation. Therefore, there are problems on the calculation side with regard to this tendency. The cause of this is the problem of the space mesh. In Q-, H- and F-calculations, the mesh point numbers for 1 lattice of 5.52 cm × 5.52 cm are 4 × 4, 4 × 2, and 2 × 2, respectively. When the eigenvalues of CQ and CF are actually compared, the F-calculation gives larger values. This is due to the fact that the F-calculation evaluated the leakage of neutrons from the core lower from the comparison of the neutron flux distribution and the fission neutron number distribution. In the calculations on these systems, the mesh interval has an effect on the evaluation of neutrons from the core and on such heterogeneous regions in the core as the sodium channels and B_4C simulating control rods and work on the eigenvalues in the positive direction and in the positive and negative direction, respectively. However, from the comparison of the eigenvalues of 2BQ and 2BF, it is seen that the values show larger changes in the system with two B_4C simulating control rods than in the clean system (Cq, CF). The mesh interval effect is so complicated that it will be further studied in 5.3.2.

Table 20 C/E-raw data

Experimental No.		calc. sys.	E % δ k/k	C % δ k/k	C/E *	symmetry
1B-	1BC	BCQ	2.52±0.04	2.60	1.03±0.02	Q
	B1	B1F	1.12±0.01	1.08	0.97±0.01	F
	B2	1BH	1.32±0.01	1.33	1.01±0.01	H
		B2F		1.30	0.99±0.01	F
4B,5B-	4B	4BQ	4.50±0.07	4.66	1.04±0.02	Q
	5B	5BH	5.86±0.10	6.03	1.03±0.02	H
Tr-	Tr-1	1BQ	2.72±0.04	2.79	1.03±0.01	Q
		2BF		2.72	1.00±0.01	F
	Tr-2	TR2Q	3.58±0.04	3.78	1.06±0.01	Q
	Tr-3	TR3Q	4.17±0.06	4.52	1.09±0.02	Q
In-	In-1	IN1F	2.49±0.03	2.45	0.99±0.01	F

Experimental No.		calc. sys.	E % k/k	C % k/k	C/E *	summary
In-	In-2	IN2F	2.41±0.03	2.35	0.98±0.01	F
	In-3	IN3F	2.11±0.06	2.11	1.00±0.03	F
Pa-	Pa-1	PA1F	2.08±0.04	2.18	1.04±0.02	F
	Pa-2	PA2F	4.42±0.07	4.69	1.06±0.03	F

* Errors in C and ρ_0 are not included.

Here, if the ratio of 2BQ and 2BF is used as a normalization factor and the reactivity worth values obtained by F-calculation is multiplied by this factor, the C/E values generally become larger, thus improving the deviation of C/E values from 1.0.

Next, looking at the C/E values classified by the experimental items, it is found that particular large deviations are observed in Tr-experiment and Pa-experiment. In Tr-experiment, we used A for V-3 clean system as was previously mentioned. This means that there was movements of fuel to and from the system on which N measurements were made and also the movement of the neutron sources. These movements were responsible for such large deviations in this experiment. This is verified by the fact that when A for the V-3 clean system is used in the experiment with 1BC containing the B_4C simulating control rod in the center the C/E values become roughly 1.10. Also considering the fact that the eigenvalues of TC2 and TC3 are sufficiently close to 1,000, it was found that there were some failures in Tr-2 and Tr-3 experiments and the values obtained by these experiments were not reliable.

The fact that the C/E values obtained in Pa-experiment were larger than those obtained in other experiments showed that there were problems with the calculated values. And the fact that such tendency appeared despite the eigenvalue of PCF is sufficiently close to 1,000 means that there were problems with the application of the effective cross section of the B_4C region. We used the effective cross section in the case where only one B_4C simulating control rod was inserted.[note)] 4B and 5B experiments also produced C/E values roughly consistent with the results of 1B-experiment in spite of the differences in the reactivity of the systems.

Note) Refer to 4.1.5.

5.2.2 Comparison of interaction factors

The uncorrected experimental and calculated values of the interaction factors and their C/E are given in Table 21.

Table 21 C/E of interaction factor f_{ij} and f_{ij} - 1

exp. no.	position i	position j	angle*)	distance (cm)	E	C	(C/E)** f_{ij}	(C/E) f_{ij}-1
In-3	16-22	20-22	50°	22.08	0.972±0.016	0.975	1.003±0.016	0.89
In-2	14-18	16-22	65°	24.69	0.993±0.011	0.988	0.995±0.011	1.71
In-1	14-18	20-22	115°	39.81	1.022±0.011	1.030	1.008±0.011	1.36
Tr-1	14-18	22-18	180°	44.16	1.034±0.011	1.047	1.013±0.011	1.38
Pa-2	14-18	22-17	180°	44.16	1.060±0.013	1.078	1.017±0.013	1.30
	14-19	22-18						

*) Angle: observed at core center.

**) Errors in C are not included.

These values generally appear to be well in agreement with one another. This is because the ratios were taken. In order to observe the interaction effect only, it is necessary to see the C/E of f_{ij}-1. The fact that f_{ij} is generally close to 1,000 suggests that even if large systematic errors are included in the experimental values, they are probably included as factors. If the C/E of f_{ij} to be discussed only with the interaction effect as a problem, further calculation efforts seem to be necessary.

5.3 Correction of raw data

5.3.1 Correction of experimental values

As for the cause of the differences between the actual experimental system and the calculation model system, there is the problem of the central gap as discussed in 3.3.1. We corrected the experimental values so that they could be compared with the calculated values.

When B_4C simulating control rod drawer is loaded in the core, the B_4C region is located in the following position. Considering the axial half of the core (half machine), the B_4C region begins from 5.7 mm away from the center surface (contacted surface).

Since the B_4C regon is 300.43 mm while the core height is 304.8 mm, the B_4C region is out of the core 1.35 mm and ends in the blanket.

Since the real weight of B_4C is retained in the calculation model, there is no need of any correction for the aforesaid fact where the importance and the neutron flux is flat, if the self-shielding effect is not taken into consideration. In order to match the real conditions with the calculation model, we considered corrections in the following three steps.

1) the whole B_4C simulating control rod is moved 1.35 mm toward the center,
2) the density of B_4C is reduced by 4.35/304.8, and
3) the center gap is filled with 4.35/304.8 B_4C.

The effect of 1) increases the reactivity worth of a simulating control rod by 0.24 % due to the stroke characteristic curve[note)] and the B_4C sample reactivity worth traverse. The effect of 2), the reduction of density, reduces the reactivity worth by 4.35/304.8 = 1.42 %. As for the effect of 3), addition of B_4C in the center. The aforesaid sample reactivity worth traverse data were used. That is to say that since B_4C had a reactivity worth of -0.00149 % $\delta k/k/g$ in the position of 14-18 and the amount of B_4C to be added in the center was 13.30 g, this effect is to increase the reactivity worth of B_4C simulating control rod by 1.53 %.

Considering the above increases and decreases in the reactivity worth of B_4C simulating control rod, it is necessary to increase the experimental value by

$$0.24 - 1.42 + 1.53 = +0.35\ \%$$

This correction factor is so small that the error in this factor is virtually negligible if the experimental errors in the experimental values are also considered.

The above value was calculated with the B_4C simulating rod inserted in the position of 14-18 and it is also inconceivable that there are any large changes in another positions where the reactivity worth of B_4C control rod was measured. For this reason, this value was used as the correction factor for all experimental values.

Note) Refer to Appendix (A8).

5.3.2 Correction of calculated values

In the preceeding paragraph, the effect of the mesh point number on the reactivity worth calculation became a big problem. Here, we made estimation of the changes in the reactivity worth values between the H- F-calculations and the Q-calculation and this correction was applied to the calculated values so that they are equivalent to the values obtained by the Q-calculation. And this calculated value was used as the correct value of reactivity worth. In actuality, however, there were not enough data on the mesh interval and effective multiplication factor and many assumptions were used and moreover the amount of correction exceeded 4 % where it was largest, thus providing the sources of calculation errors.

The increase in the mesh interval results in a change in the calculated value of neutron flux distribution and consequently in the effective multiplication factor. So, the increase in the mesh interval is studied by comparing with the change in the reactivity of the system on which the calculation was made. This can be said to be appropriate from the standpoint of the variational principle, too. In the Q-, H- and F-calculations, double calculations were made in CQ, CH and CF of the system (CL) without B_4C simulating control rod and in 1BH and B2F of the system (1B) with one B_4C simulating control rod, and in 2BQ and 2BF of the system (2B) with two B_4C simulating control rods. They are shown in Table 22.

The changes of Q → F in 2B system and those of H → F in 1B system were compared. Considering this, we assumed that the changes of Q → H → F in 1B and 2B systems were compared with those in CL system. Thus estimated changes of Q → H in 1B system and those of Q → H and H → F in 2B system are given in brackets in Table 22.

Table 22 Reactivity change due to mesh interval

$10^{-4}\ \delta\ k/k$

System	H → Q	F → H	F → Q
CL	3.603	6.284	9.887
1B	(5.347)	9.326	(14.673)
2B	(6.154)	(10.732)	16.886

Q : 4 × 4 meshes/lattice
H : 4 × 2 meshes/lattice
F : 2 × 2 meshes/lattice

From this table, it is seen that the changes of Q → H are about a half of those of H → F, showing a remarkable converging tendency. In the direction of CL → 1B → 2B, the tendency for the changes to increase slows down greatly. This phenomenon probably indicates that the negative element grows in the offsetting of positive and negative elements mentioned in the preceding paragraph as the number of B_4C simulating control rods increases or probably it should be considered the differences between 1B and 2B are reflected in the neutron flux distribution and its symmetry, judging from the fact the mesh interval influences the neutron flux distribution.

It is extremely difficult to estimate the amounts of corrections to be made to the calculated values which require correction according to the neutron flux distribution condition. So, we assumed that the amounts of corrections depend on the number of B_4C simulating control rods contained the system regardless of the neutron flux distribution condition (the positions of B_4C simulating control rods). It is impossible to estimate the amount of correction in the case of 5HB and PA2F. However, as was discussed before, if the negative element grows as the number of B_4C simulating control rods increase, the amount of required correction becomes smaller than in the case of 2B and it is also conceivable that the symbol is reversed. In this case, however, the reactivity worth itself is so large that the amount of correction presumably assumes a small percentage. So, as for 5BH and PA2F, we decided to use the correction value of H → Q and F → Q in the 2B system.

On the basis of the above superposition, the amounts of differences between CL system and 1B or 2B system were regarded as the amounts of corrections and thus corrected calculated values are given in Table 23. Looking at these corrected calculated values, it is seen that $4B/4 \times B1 = 0.996$ and $5B/(4 \times B1 + B2) = 1.03_2$, showing large deviations from their uncorrected values of 1.077 and 1.071 (or 1.065). The interaction factors calculated by use of the corrected calculated values are given in Table 24. These f_{ij} values are generally smaller than the uncorrected ones. From the fact the F-calculated values were used consistently for the calculation of the uncorrected interactions, it is expected for the uncorrected interaction factors that the mesh interval effect is offset to some extent, and in this respect this is not necessarily meaningless.

Table 23 Mesh number correction to calculated rod worth

no. system	uncorrected worth % δ k/k	correction % δ k/k	corrected worth % δ k/k
1BH	1.330 70	0.017 44	1.348 14
5BH	6.026 74	0.025 53	6.052 27
IN1F	2.453 23	0.069 98	2.523 21
IN2F	2.353 61	0.069 98	2.423 59
IN3F	2.108 66	0.069 98	2.178 64
TR1F	2.722 70	0.069 98	2.792 68
B1F	1.081 59	0.047 86	1.129 45
B2F	1.300 28	0.047 86	1.348 14
PA1F	2.175 86	0.069 98	2.245 84
PA2F	4.691 85	0.069 98	4.761 83

However, the fact that the ratios between the calculated values change so much by such estimated corrections is indicative of the limit to the reliability of the calculated values and further efforts are required for the calculation of the interaction factors. Such being the case, importance is to be attached to the relationship between the reactivity worth in each case and the corresponding experimental value. In this case, the ratio between the calculated values is not taken and accordingly their arises no accumulation of calculation errors.

Table 24 Interaction factor f_{ij} with corrected calculation values

exp. no.	position		angle	distance (cm)	uncorrected f_{ij}	corrected f_{ij}
	i	j				
In-3	16-22	20-22	50°	22.08	0.975	0.965
In-2	14-18	16-22	65°	24.69	0.988	0.950
In-1	14-18	20-22	115°	39.81	1.030	0.990
Tr-1	14-18	22-18	180°	44.16	1.047	1.036
Pa-2	14-18	22-17	180°	44.16	1.078	1.060
	14-19	22-18				

* Angle: observed at core center.

As discussed above, we performed the operation to covert all the values of reactivity worths equivalent to the values obtained by the Q-calculation. However, it is not known for sure how much more correction would be required if the mesh point number is increased infinitely. But, judging from the tendency of the amounts of corrections of H Q as seen in Table 22, and the diffusion factor of the system and the mesh interval (1.38 cm) in the Q-calculation, the amount of correction presumably does not exceed 1 % at least in the case of 1B and 2B.

5.4 Secondary comparison (C/E Corrected)

The corrected experimental and calculated values, which were discussed in the preceding paragraph, and their C/E are given in Table 25. The C/E values have a good consistency and shows no systematic tendency. The additivity of the reactivity worth in experimental and calculated values has been established by the previous made study.

The fact that the C/E values exceed 1.00 suggests a limit to the diffusion approximation calculation. With regard to an example by S_4 calculation,[14] it is said that this effect tends to make the calculated values 4 % lower. If this is true, then it follows that C/E values are smaller than 1.00 and the experiments see large reactivity worths. In the V-3 clean system, the calculated value of eigenvalue was obtained with a good accuracy but the calculated value is not necessarily reliable when such a new substance as B_4C is used, and it cannot be generally said that the experimental values are systematically too large.

There are problems with the accuracy of the chemical quantitative determination of B_4C. As for the sintered pellets of B_4C which were used in our experiments, there are the data of measured values obtained in Japan[note)] apart from the data prepared by PARTIOT. According to these data, the amount of B^{10} would decrease by -1.37 % and the C/E would also show a similar movement. As for the measurements made in Japan, the chemical analysis and isotopic analysis were performed at different organization.

In the calculation of the kinetic parameters, if the source data for β_i^m are changed and Keepin's data are used, ρ_0 becomes about

Note) Refer to Appendix (A9)

2 % smaller and consequently the experimental values become smaller and the C/E values become so much larger.

Table 25 Rod worth C/E-corrected

experimental No.		rod position	E %δk/k	C %δk/k	C/E *
1B-	1BC	18-18	2.52±0.04	2.60	1.03±0.02
	B1	16-22	1.12±0.01	1.13	1.02±0.01
	B2	14-18	1.32±0.01	1.35	1.01±0.01
4B,5B-	4B	16-14 16-22 20-14 20-22	4.51±0.07	4.66	1.03±0.02
	5B	16-14 16-22 20-14 20-22 14-18	5.87±0.10	6.05	1.03±0.02
Tr-	Tr-1	14-18 22-18	2.73±0.04	2.79	1.02±0.01
	Tr-2	15-18 21-18	3.59±0.04	3.78	1.05±0.01
	Tr-3	16-18 20-18	4.18±0.06	4.52	1.08±0.02
In-	In-1	14-18 20-22	2.49±0.03	2.52	1.01±0.01
	In-2	14-18 16-22	2.42±0.03	2.42	1.00±0.01
	In-3	16-22 20-22	2.11±0.06	2.18	1.03±0.03
Pa-	Pa-1	14-18 14-19	2.09±0.04	2.25	1.07±0.02
	Pa-2	14-18 14-19 22-17 22-18	4.43±0.08	4.76	1.08±0.03

* Errors in C and ρ_0 are not included.

The cross section of B^{10} note) has not been determined with particularly good accuracy. And the C/E values of the sample reactivity worth in the center are not well in agreement. When

Note) In the case of one-dimensional 25-group calculation, when the central drawer is replaced with a sodium channel, if the calculations are made by J.F-II and ABBN, the reactivity change becomes 0.752 % k/k and 0.719 % k/k, respectively. If it is replaced with one-rod type B_4C, the calculated values become 2.523 % k/k and 2.261 % k/k, respectively. (This is the calculation on a model and does not mean the reactivity worth of the actual one-rod type). It is needless to say that this difference is caused by the difference in all cross sections of B-10 but the differences in C/E by the cross section set exceed the range of experimental errors.

sodium is replaced with B_4C, B_z^2 also changes. This B_z^2 was obtained from the amount of neutrons leaking the boundary between the core and blanket in the radial direction. However, the diffusion calculation method is not suited for grasping such phenomena in the boundary. We assumed an isotropic scattering in the collision probability method for obtaining the effective cross section of 7-pin cluster but the actual angular distribution of neutron flux is presumed to have a very strong anisotropy.

6. Conclusion and problems to be solved in the future

6.1 Conclusion

1) The criticality of V-3 assembly system containing no B_4C simulating control rod showed well agreed values for k_{eff} obtained by the homogeneous two-dimensional diffusion calculation, using the JAERI-FAST version II 8-group collapsed cross sections, coming roughly within -0.3 % δk/k.
2) The C/E values of the reactivity worth of B_4C simulating control rods generally had a consistency without any correlation with the reactivity of the system.
3) Tr-2 and Tr-3 showd values largely deviated from others. It was found that this was because the experimental values were not reliable.
4) As for the interaction effect of two B_4C simulating control rods, the experimental and calculated values showed an identical tendency.
5) The additivity of the reactivity worths when many B_4C simulating control rods were symmetrically distributed in the core was established within the range of the errors in the experiments and calculations up to the -6 % δk/k sub-critical system.
6) As for the analysis of the results of Pa-experiment, it is necessary to prepare the effective cross section of B_4C simulating control for the analysis.
7) When the counters are located considerably removed from the core in the case of the neutron multiplication method, the effective multiplication factor of the system to be observed is largely dependent on the neutron source distribution condition at the time of A measurement than on the counter positions.
8) When the mesh interval is gradually widened in the case of the diffusion calculation method, the calculated reactivity worths grow smaller if one or two B_4C simulating control rods are inserted in the system.

6.2 Problems to be solved in the future

The presence of B_4C simulating control rods in the core bring about great difficulties in experiments and calculations. However, even in the case of a system containing B_4C simulating control rod, the experimental values (effective multiplication factor or reactivity of the system) are determined when the system in a critical state. Such being the case, it is possible to check the reliability of the calculated first eigenvalue of the system containing B_4C simulating control rod by comparing the results of calculation on this system with the results of calculation made on a clean system. This is related to the checking of the reliability of the calculated value of reactivity worth and to the checking of the neutron source multiplication method. As for V-3 assembly, when one or two B_4C simulating control rods are inserted, we have the experimental values obtained by filling other sodium channels with fuel. It is necessary to make calculations on these systems.

To compare with the results of other experimental methods such as the pulsed neutron method and the critical method is more direct and useful in the analysis of the values measured by the respective methods.

In the case of the neutron source multiplication method, the knowledge to know the position dependency of the effective multiplication factor the system to be measured has a great effect on the experimental plan and accuracy. A study in this field is an important subject of study in the future.

We thicks it a necessary process of checking to obtain the reactivity worths by other group constants and calculation codes. The calculation of the interaction factor must be carefully done by making the most effective calculation system for the purpose.

Acknowledgement

We wish to express our gratitude to the staff of the Fast Reactor Physics Laboratory for their valuable cooperation. We are indepted to Mr. Toru Hiraoka and Mr. Masabumi Nakano of the same laboratory for their participation in the very useful discussion during our experiments. We also are grateful to Mr. Tomoo Suzuki

6.2 Problems to be solved in the future

The presence of B_4C simulating control rods in the core bring about great difficulties in experiments and calculations. However, even in the case of a system containing B_4C simulating control rod, the experimental values (effective multiplication factor or reactivity of the system) are determined when the system in a critical state. Such being the case, it is possible to check the reliability of the calculated first eigenvalue of the system containing B_4C simulating control rod by comparing the results of calculation on this system with the results of calculation made on a clean system. This is related to the checking of the reliability of the calculated value of reactivity worth and to the checking of the neutron source multiplication method. As for V-3 assembly, when one or two B_4C simulating control rods are inserted, we have the experimental values obtained by filling other sodium channels with fuel. It is necessary to make calculations on these systems.

To compare with the results of other experimental methods such as the pulsed neutron method and the critical method is more direct and useful in the analysis of the values measured by the respective methods.

In the case of the neutron source multiplication method, the knowledge to know the position dependency of the effective multiplication factor the system to be measured has a great effect on the experimental plan and accuracy. A study in this field is an important subject of study in the future.

We thicks it a necessary process of checking to obtain the reactivity worths by other group constants and calculation codes. The calculation of the interaction factor must be carefully done by making the most effective calculation system for the purpose.

Acknowledgement

We wish to express our gratitude to the staff of the Fast Reactor Physics Laboratory for their valuable cooperation. We are indepted to Mr. Toru Hiraoka and Mr. Masabumi Nakano of the same laboratory for their participation in the very useful discussion during our experiments. We also are grateful to Mr. Tomoo Suzuki

of the Nuclear Design Laboratory and Mr. Keiichi Tsuchihashi of the Reactor Physics Laboratory for their assistance in calculations.

Bibliography

(1) Naohiro Hirakawa, et al.: "FCA V-1 Assembly Characteristics Test and Critical Mass" (1970); Private communication

(2) Tsutomu Iijima, et al.: "FCA V-2 Assembly Characteristics Test and Critical Mass" (1971); Private communication

(3) Keeping G.R.: "Physics of nuclear kinetics", Addision-Wesley (1964)

(4) Davey W.G. et al.: "Techniques in fast reactor critical experiment", Gordon and Breach (1970)

(5) Nobutatsu Mizoo and others: "Collection of manuscript papers for the nuclear reactor physics sectional meeting in 1971", B32 (1971)

(6) Usacheff L.N.: "Proceedings of 1st Geneva Conference", 5. 503 (1956)

(7) Katsuragi S. et al.: "JAERI-Fast Reactor Group Constants System", Part I, II, JAERI-1195 (1970) and 1199 (1970)

(8) Tomoo Suzuki: "Fast Reactor 1-Dimensional Diffusion Code (EXPANDA-4) using JAERI-FAST SET", JAERI-memo 3660 (1970)

(9) Keiichiro Tsuchihashi: "PIJF collision probability program for calculation of multi-group neutron flux distribution", JAERI-memo 2985 (1968) and "Program for calculation of the multi-region multi-group collision probability of CLUP cluster lattice", JAERI-memo 3034 (1968)

(10) Fowler T.B. et al.: "Nuclear reactor core analysis code CITATION", ORNL-TM-2497 (1969).

(11) Sandmeir H.A.: ANL-6423 (1961)

(12) Koji Ikawa: (1971), Private communication

(13) Nobutatsu Mizoo, et al.: Manuscript papers for 1972 annual meeting (1972)

(14) Shungo Iijima, et al.: Manuscript papers for 1971 nuclear reactor physics sectional meeting, B12 (1971)

APPENDICES

Appendix (A1): Core drawer drawings

The fuel and control rod drawer loading of V-3 assembly is exactly the same as V-2. The core and rod drawer loadings are illustrated in Fig. A1-1 and Fig. A1-2, respectively. Pu is 90.0 - 91.2 w/o ^{239}Pu and Eu is 20 w/o enriched ^{235}U.

Appendix (A2): Position dependence of subcriticality

The dependence of the subcriticality to be observed on the counter positions is graphically shown in Fig. A2. The distances from the core center to the counters are on the horizontal axis and the deviations of the subcriticality from the average value are on the vertical axis. The values are scattered roughly within the measuring accuracy when the subcriticality is most shallow, $3.33\,\rho_o$ ($0.12\,\%\,\delta$ k/k). As the subcriticality grows deeper, the scattering of the values become larger and they have a systematic tendency. However, they showed a tendency to converage even where the subcriticality is deepest, $155\,\rho_o$ ($5.5\,\%\,\delta$ k/k) and even the most widely scattered values are within the accuracy range of ± 10 %. 4B and 5B in the figure indicate the core patterns, not the reactivity worth thereof.

Appendix (A3): Comparison of averaging operations

Table 3 shows the average values and their standard deviation differences in various core patterns and subcriticalities. The values under A-method were obtained with regard to a certain A, not the average value of A in various cases. The values given besides 14-18, 4B, 5B and so forth in the table do not represent their reactivity worths. 14-18, 4B, 5B and so forth can be considered as meaning the core patterns.

From this table, it is seen that the $\delta\rho$-method alwasy gives larger values than the A-method and the errors grow larger sharply when the subcriticality become deep. In the A-method, the average values of three kinds do not show large changes but when R^2 weighed the standard deviations become considerably small, suggesting a saturating tendency where removed from the core. 14-18 and Pa-1 are nearly the same in the core pattern but their singularity

Table A3 Subcriticality and weighting method

(ρ_0)

B_4C rod position	A-method			$\delta\rho$-method
	equi-	σ^{-2}	$\sigma^{-2}.R^2$	$\sigma^{-2}.R^2$
14-18	36.91±0.26	36.89±0.29	36.84±0.13	39.07±0.18
4B	123.42±0.96	124.72±0.93	123.66±0.62	134.03±2.17
5B	162.1 ±2.2	163.4 ± 2.2	161.8 ±1.1	186.2 ±4.2
In-3	59.62±0.98	60.51±0.53	60.50±0.45	62.02±0.60
Tr-1	76.59±1.05	78.68±0.80	75.96±0.35	83.16±0.86
Pa-1	59.09±0.76	58.68±0.84	59.11±0.35	63.54±0.73

equi-; equi-weighting, σ^{-2}; precison weighting, $\sigma^{-2}\cdot R^2$; precision and R^2 wighting where R means the distance between a counter and core center.

intensities are different slightly less than two times. In this case, no difference is observed in the tendencies of average values between the three kinds of averaging operations but the standard deviations are extremely large and the relative errors are roughly two times larger.

Appendix (A4): Collapsing effect survey

We made calculations on the V-3 clean core (CL1) and the core (BC1) containing a B_4C simulating control rod (one-rod type) in the center by EXPAND-4, using the 25-group set of JAERI-FAST Version II. The calculations systems were one-dimensional cylinders and the space mesh regions and their B are given in Table A4-1. In order to determine the kind of group collapsing, we referred to $\sigma_f^{core}(E_i)\phi(E_i)$, $\sigma_a^{core}(E_i)\phi(E_i)$ and $\sigma_a^{B10}(E_i)\phi(E_i)$ of FCA V-2 assembly (similar to V-3 in structure). As a result, we decided to survey the 10 kinds of groups as shown in Fig. A4-1. The calculated values of the effective multiplication factor are given in Table A4-2.

In the extreme right column are given the reactivity worths in the center of one-rod type B_4C simulating control rods.[note)]

Note) These values were obtained by calculations on a model and they are not to be compared directly with experimental values.

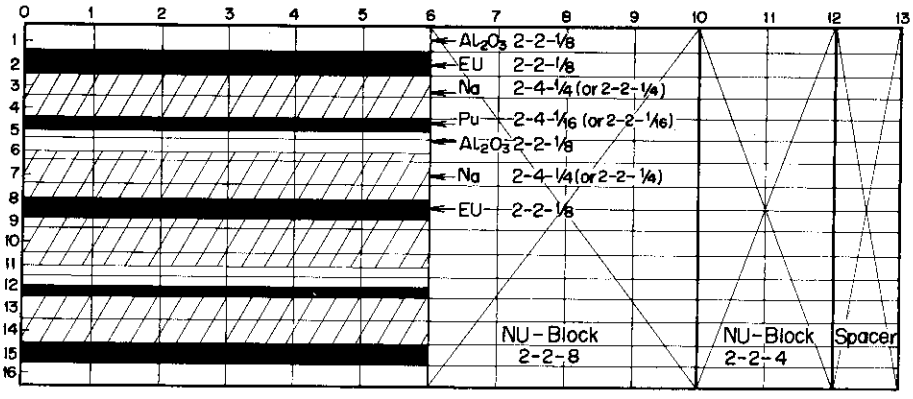

Fig. A1-1 Top view of assembly V-3 core drawer loading

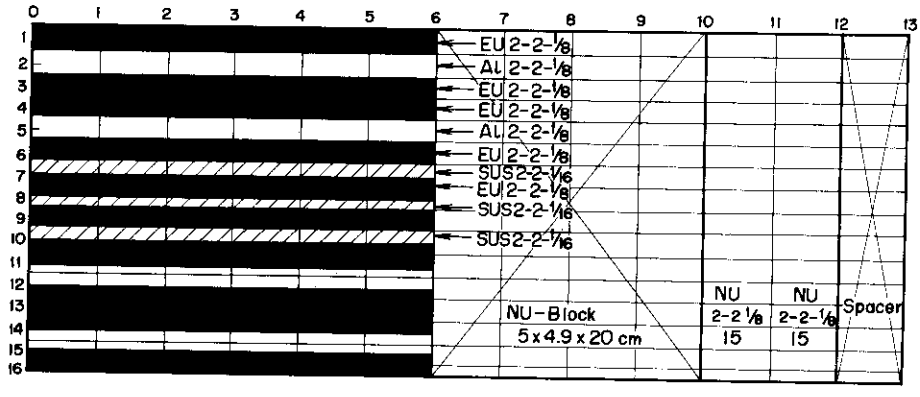

Fig. A1-2 Top view of assembly V-3 control and safety drawer loading

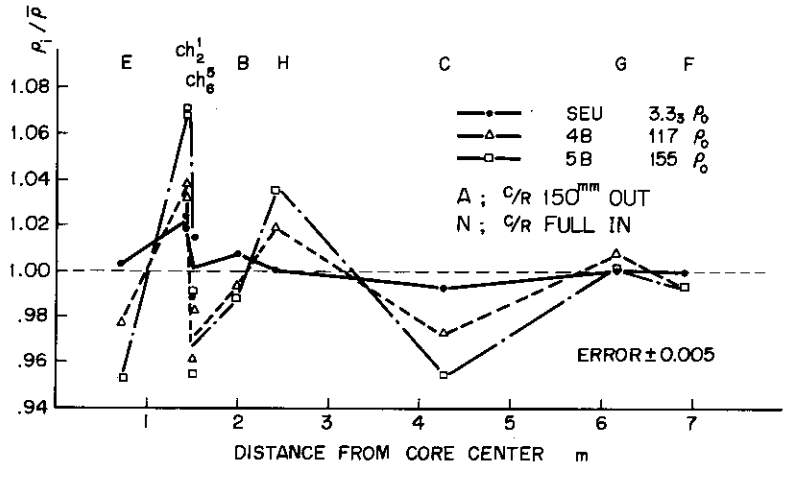

Fig. A2 Position dependence of subcriticality

The values of reactivity worth are little dependent on the collapsing group number and the way of collapsing and it is presumed that k_{eff}^{CL1} and k_{eff}^{BC1} have a very good parallelism. Such being the case, not much difference arises whichever collapsed group you may use.

Table A4-2 Calculated eigenvalues of CL1 and BC1 for various group collapsing using the one dimensional cylindrical model.

NG	k_{eff}^{CL1}	k_{eff}^{BC1}	$\frac{k_{eff}^{CL1} - k_{eff}^{BC1}}{k_{eff}^{CL1} \cdot k_{eff}^{BC1}}$ *)
25	1.00098322	0.96918640	0.0327755
12	1.00074348	0.96888251	0.0328598
10	1.00052760	0.96866089	0.0328803
8	1.00055822	0.96867480	0.0328961
8'	1.00168271	0.96980095	0.0328193
7	1.00177570	0.96987368	0.0328346
6	1.00271415	0.97073273	0.0328564
6'	1.00170259	0.96980065	0.0328394
6"	1.00234828	0.97036863	0.0328789
5	1.00555777	0.97353767	0.0327080
4	1.00260686	0.97087086	0.0326031

*) This value represents the reactivity worth of the one rod type B_4C at the center of the core.

Since this survey is not so sensitive to the differences of such overall quantities as the effective multiplication factors when they are compared, we watched the differences with regard to the quantities relating to the neutron flux distribution pattern. For this purpose, we plotted the quantities which can be expressed by the following equation as the function of the distance from the core center.

$$R^{NG}(r) = \sum_{i=1}^{NG} \Sigma_{ai}^{B_4C}(r=0)\,\phi_i(r) \Big/ \sum_{i=1}^{25} \Sigma_{ai}^{B_4C}(r=0)\,\phi_i(r)$$

(Calculated from the values obtained by BC1 calculation)

From this graph it is seen that NG - 12, 10 and 8 resemble one another in behavior and relatively close to NG = 25 while NG = 7 and 6 are far apart. Since the smallest group number among those

Table A4-1 Models for 1-dimensional cylindrical survey calculation

Assy.	R cm 0.0	1.45	3.1143	6.2286	19.3200	28.4151	35.3722	44.8817	63.9007
BC1	Material	B_4C	Na	core	core	core+Na	core	blanket	blanket
	Δr(Mesh no)	0.3625 (4)	0.41608 (8)	0.51905(14)	0.65457(34)	0.75793(46)	0.86964(54)	0.95095(64)	0.95095(84)
	$B_Z^2 \times 10^3$	0.3534	0.8115	1.1784	1.1784	1.1784	1.2431	1.2963	1.0548
NC1	Material	Na		the same as above	the same as above	the same as above	the same as above	the same as above	the same as above
	Δr(Mesh no)	0.51905 (6)		0.51905(12)	(32)	(44)	(52)	(62)	(82)
	$B_Z^2 \times 10^3$	0.8115							
CL1	Material	core			the same as above	the same as above	the same as above	the same as above	the same as above
	Δr(Mesh no)	0.51905(12)			(32)	(44)	(52)	(62)	(82)
	$B_Z^2 \times 10^3$	1.1784							

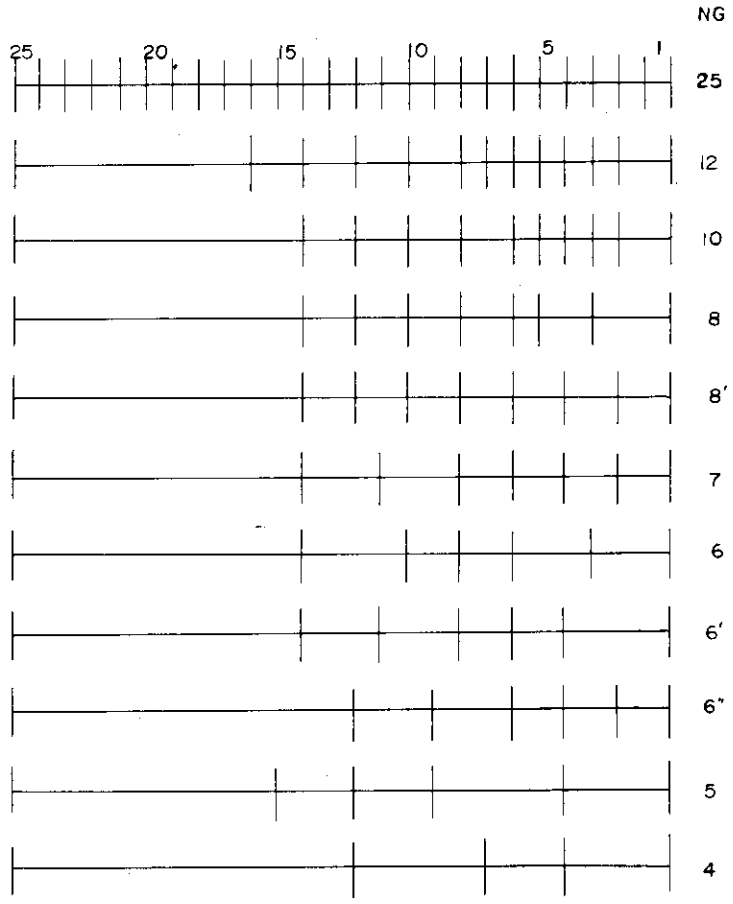

Fig. A4-1 Group collapsing

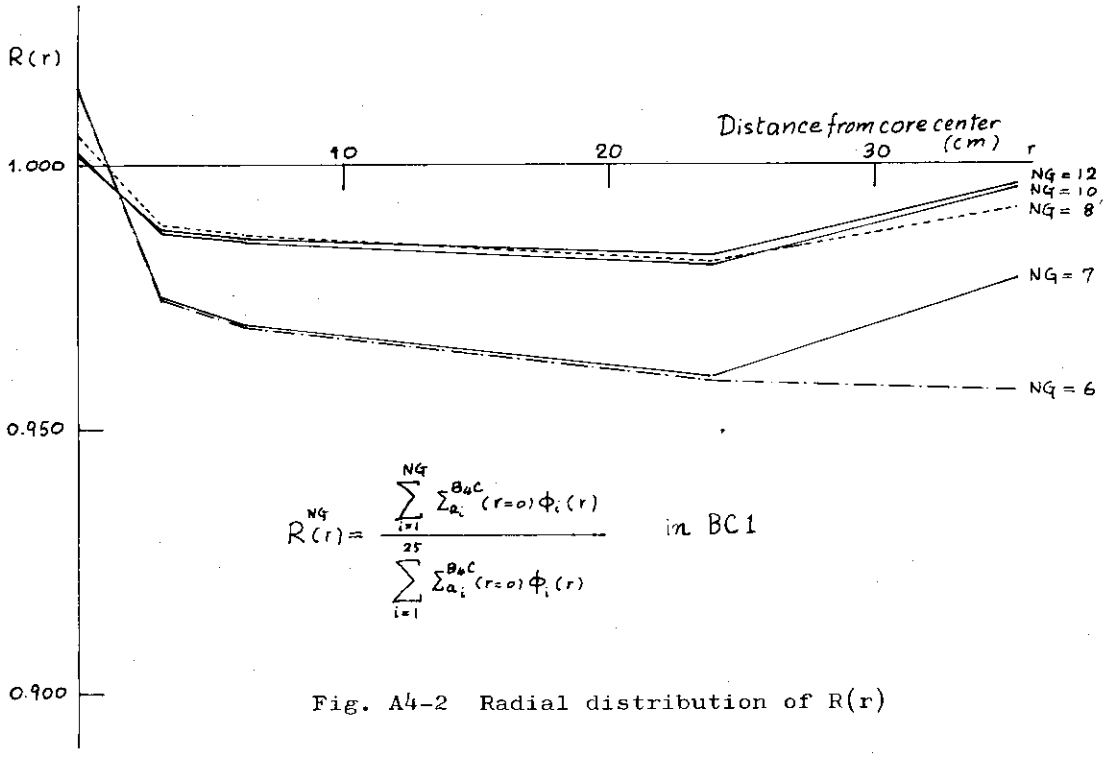

Fig. A4-2 Radial distribution of R(r)

Table A4-3 $\sum_{i=1}^{NG} S_i(r) / \sum_{i=1}^{25} S_i(r)$ from CL1 calculation

r / NG distance from core center	25	12	10	8'	6'
3.11 cm	1.000000	1.000334	1.000792	1.000606	1.000424
6.23	1.000000	1.000392	1.000869	1.000706	1.000644
23.87	1.000000	0.999728	0.999553	1.000123	0.999931
35.37	1.000000	1.000562	1.000351	0.991013	0.993869

Table A4-4 Zone integrated Source from CL1 calculation

Zone No.	25	10	8'	6'
1	0.0	0.0	0.0	0.0
2	0.0	0.0	0.0	0.0
3	1.000000	1.000576	1.000579	1.000253
4	1.000000	1.000270	1.000480	1.000276
5	1.000000	0.999634	1.000230	1.000106
6	1.000000	0.999519	0.999740	0.999842
7	1.000000	1.001026	0.998982	0.999808
8	1.000000	1.001346	0.996962	0.997423

Table A4-5 Group collapsing effect on control rod interaction factor f

B_4C rod distance : 11.00cm, core length : 33.92 cm

NG	25	10	8'	6'	$B_\perp^2$
Ref	1.00333218	1.00319850	1.00368635	1.00375346	2.05×10^{-3}
$1B_4C$	0.99204513	0.99166637	0.99184583	0.99190608	-1.06×10^{-2}
$2B_4C$	0.98282579	0.98232478	0.98235846	0.98227435	-1.06×10^{-2}
ρ_1	0.01133977	0.011725645	0.011894017	0.011899390	
ρ_2	0.02079543	0.02118156	0.02163116	0.02178494	
f	0.916925	0.9136307	0.909329	0.915381	

B_4C rod distance : 24.54 cm, core length : 43.65 cm

NG	25	10	8'	6'	$B_\perp^2$
Ref	0.99259936	0.99250487	0.99304689	0.99315386	2.05×10^{-3}
$1B_4C$	0.98566339	0.98550133	0.98594479	0.98598874	-9.30×10^{-3}
$2B_4C$	0.97148590	0.97120894	0.97164230	0.97158343	-9.30×10^{-3}
ρ_1	0.007089	0.007160	0.007253	0.007316	
ρ_2	0.021894	0.022092	0.022183	0.022354	
f	1.5442	1.5427	1.5292	1.5277	

which show a similar behavior should be adopted, NG = 8 is considered to be most appropriate.

In order to see the effects of the group collapsing on the distribution system, we checked the changes of the source standardized by several radial points, that is, $\sum_{i=1}^{NG} Si(r) / \sum_{i=1}^{25} Si(r)$ as shown in Table A4-3. Table A4-4 shows the standardized source integrated by the region, that is, $\sum_{i=1}^{NG} \sum_{j} S_i \Delta V_j / \sum_{i=1}^{25} \sum_{j} Si\ \Delta V_j$. As far as these values are compared, almost no effect of the group collapsing is observed.

Next, we made the following checking calculation because it was conceivable that the group collapsing influences the propagation of the neutrons in the system and it has a particularly large effect on the calculation of the interaction factor of B_4C simulating control rod. We set the B_4C simulating control rod region at the actual thickness (5.52 cm) and the traverse buckling of the region at an appropriate negative value to make a hypothetical system of subcriticality. Using this system, we made calculations by the 25, 10, 8 and 6 groups in two different cases, that is, when one B_4C simulating control is inserted in the system and when two rods are inserted and compared the calculated values in the form of the interaction factor ($f_{12} = \delta\rho\ (1,\ 2) / \{\delta\rho\ (1) + \delta\rho(2)\}$). (Refer to Table A4-5) As seen from Table A4-5, if the value of f by 25-group calculation is taken as a standard, the values obtained by any collapsed group calculation are within 1 % and therefore there is no need of taking into consideration the effect of group collapsing on the interaction factor.

As a result of the above overall survey calculations, we decided to adopt 8 groups for the two-dimensional calculations in the present analytical study.

Appendix (A5): Other surveys

A5.1 Buffer region

We checked the effect of the presence of buffer region on k_{eff} by one-dimensional calculation (EXPANDA-4). The survey was made by using 25 groups and 8 groups in the four cases as shown in Fig. 25.1-1. Buffer - 1 is located near B_4C to adop the effect of the spectrum hardening. Buffer - 2 adopts the changes in the spectrum near the boundary between the core and blanket. The k_{eff} values in

the respective case are given in Table A5.1-1.

Table A5.1-1 Results of buffer survey calculation

Buffer - 1	Buffer - 2	k_{eff}	
		25G	8G
+	+	0.969 186 40	0.969 800 95
+	-	0.968 988 05	0.969 672 46
-	+	0.969 240 05	0.969 837 05
-	-	0.970 117 56	0.970 802 27

If a certain k_{eff} value of Buffer-1 and -2 is considered as a standard, from this table it is seen that the changes in k_{eff} when Buffer-2 is removed (+0.013 % for 8 groups and +0.02 % for 25 groups) are considerable large as compared with those when Buffer-1 is removed (-0.003 % for 8 groups and -0.005 % for 25 groups).

A5.2 Effects of fission spectrum χ_i

The calculated values (eigenvalues and reactivity worths) obtained by the one-dimensional basic system with 8 groups, using $\chi_i(Pu^{239})$ and $\chi_i(U^{235})$ (refer to Table A5.2-1) are shown in Table A5.2-2. The calculated values obtained by using χ_i of Pu^{239} and those which were obtained by using χ_i of U^{235} showed differences of about 1 % in the form of B_4C reactivity worth. So, in the two-dimensional 8-group calculation, we used the average value of χ_i weighted by the neutron number ($\upsilon^{25}\Sigma_f^{25} + \upsilon^{49}\Sigma_f^{49}$) of Pu and U actually produced by nuclear fission. (The bottom row in Table A5.2-1)

$$\chi_{jav} = \frac{\chi_j^{25} \sum_{i=1}^{8} (\nu\Sigma_f)_i^{25} \phi_i + \chi_j^{49} \sum_{i=1}^{8} (\nu\Sigma_f)_i^{49} \phi_i}{\sum_{i=1}^{8} [(\nu\Sigma_f)_i^{25} + (\nu\Sigma_f)_i^{49}] \phi_i} \qquad j = 1,2,\ldots\ldots 8$$

Table A5.2-1 χ_i for Pu^{239}, for U^{235} and averaged χ_i

i	1	2	3	4	5	6	7	8
$\chi_i(Pu^{239})$	0.1137	0.4436	0.3441	0.0879	0.0102	0.0005	0.0	0.0
$\chi_i(U^{235})$	0.1047	0.4539	0.3433	0.0848	0.0123	0.0010	0.0	0.0
χiav *	0.1090	0.4490	0.3437	0.0862	0.0113	0.0008	0.0	0.0

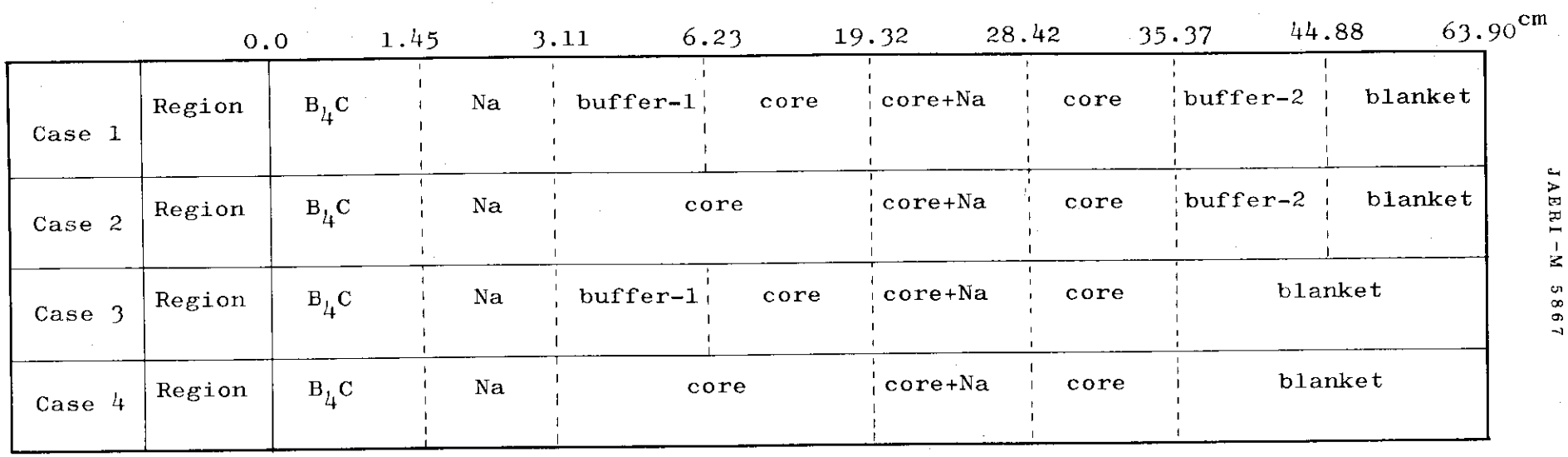

Fig. A5.1-1 Models for buffer survey calculation

Table A5.2-2 k_{eff}'s using $\chi_i(Pu^{239})$ and $\chi_i(U^{235})$

	k_{eff}(CL1)	k_{eff}(BC1)	ρ %$\delta k/k$
χ_i (Pu^{239})	1.001 682 71	0.969 800 95	3.2819
χ_i (U^{235})	1.000 983 22	0.969 395 49	3.2553

A5.3 Space mesh effect

In order to determine the positions of B_4C simulating control rods in the system, it is necessary to make X-Y two-dimensional calculation. Although the CITATION code is variable dimensions, if 8 groups are used the mesh number is restricted to about $40 \times 40 \sim 50 \times 50$.

Here we took the 8-group 84-mesh one-dimensional calculation as a standard to study the effect of the number of meshes on k_{eff} by varying the number of meshes in various regions. For this survey, we used a V-3 assembly containing 1-rod type B_4C simulating control rod in its center. The particulars relating to the region and mesh number are given in Table A5.3-1. The following things may be said qualitatively from this table.

a) If the mesh number in the regions other than B_4C in the center of the system and sodium is about 1/2 mesh (76 meshes → 42 meshes), the k_{eff} value slightly increases compared with the standard calculation.

b) If the mesh number in the B_4C region is 1/2 mesh (4 meshes → 2 meshes), k_{eff} decreases (about 0.018 %). This is presumably because as a result of the increased mesh size in the B_4C region the neutron flux is unable to lower and consequently the B_4C reactivity worth is estimated higher.

c) If the mesh number of the sodium region adjacent to the B_4C region is 1/2 (4 meshes → 2 meshes), k_{eff} increases (about 0.087 %).

d) As far as this survey is concerned, the calculability of the effect of the mesh number of k_{eff} is very good.

Appendix (A6): Calculation of B_z^2

The system which was used for the calculation is illustrated in Fig. 10 and Fig. 11. The amount of neutrons[10] leaking outward from extended plane of the end surface of the core perpendicular to

the Z axis is given by the following equation.

$$L(r)=\frac{S}{N}\ \frac{2}{\frac{\Delta Z_i}{D_i}+\frac{\Delta Z_o}{D_o}}\ [\phi(r,Zi)-\phi(r,Zo)],$$

where S is surface area, N is the number of divisions (in CITATION R mesh is divided into sections with equal volumes), D_i, ΔZ_i; D_o and ΔZ_o are the diffusion coefficients and mesh intervals on the inside and outside of the plane, respectively, and $\phi(r, Z_i)$ and $\phi(r, Z_o)$ are the values of the neutron flux at the points Z_i and Z_o on the inside and outside of the plane at the point r on the diameter.

If L(r) is integrated by r for an arbitrary region, the number of neutrons leaking outward from the region is obtained. Since this quantity ought to be equal to $\int D_i B_z^2 \phi\, dV = D_i B_z^2 \bar{\phi} \cdot V$,

$$B_z^2 = \frac{\sum L(r)}{D_i \bar{\phi} V}$$

B_z^2 can be obtained from above equation.

Appendix (A7): Comparison of kinetic parameters between 8-group two-dimensional calculation and 25-goup one-dimensional calculation

The results of survey calculations of the kinetic parameters by 8-group two-dimensional calculation and 25-group one-dimensional calculation are shown in Table A7. CL, 2B and 4B indicate that the number of B_4C simulating control rods inserted in the system is 0, 2 and 4, respectively. These are the values obtained by calculations on a model, not the values of an actual V-3 assembly.

In the case of small-group calculations, there are problems with the evaluation of the threshold fission of U-238 and the delayed neutron spectrum χ_d. One-dimensional calculation is unable to faithfully adopt the shape of the system. In the case where the system is so complicated in shape as V-3 assembly, one-dimension calculation model has problems with the evaluation of the changes in the volume ratio of the core and blanket and the flow of neutrons into the blanket. This will have an effect on the fission yield of U-238 and consequently on the evaluation of β_{eff}.

Table A5.3-1 Models is for mesh survey calculations and resulting k_{eff}'s

No.	NG	Total Mesh Number	Numbers of mesh intervals in each region, Δr(cm) in parenthesis								k_{eff}
			B_4C	Na	Buffer-1	Core	Core+Na	Core	Buffer-2	Blanket	
1	25	84	4(0.363)	4(0.416)	6(0.519)	20(0.655)	12(0.758)	8(0.870)	10(0.951)	20(0.951)	0.969 186 40
2	8	84	"	"	"	"	"	"	"	"	0.969 800 95
3	25	50	4(0.363)	4(0.416)	4(0.779)	8(1.636)	6(1.516)	8(0.870)	8(1.189)	8(2.377)	0.969 318 59
4	8	50	"	"	"	"	"	"	"	"	0.969 932 12
5	8	48	2(0.725)	"	"	"	"	"	"	"	0.969 753 13
6	8	48	4(0.363)	2(0.832)	"	"	"	"	"	"	0.970 801 81
7	8	46	2(0.725)	"	"	"	"	"	"	"	0.970 621 51
8	8	48	4(0.363)	4(0.416)	"	"	"	6(1.160)	"	"	0.969 931 96
9	8	48	"	"	"	"	"	8(0.870)	6(1.585)	"	0.969 779 91
10	8	48	"	"	"	6(2.182)	"	"	8(1.189)	"	0.970 251 79
11	8	40	2(0.725)	2(0.832)	"	"	"	6(1.160)	6(1.585)	"	0.970 779 10
			0.0	1.45	3.11	6.23	19.32	28.42	35.37	44.88	63.90

Table A7 Comparison of kinetic parameter between 1- and 2-dimensional calculation

Assembly		2-dim 8G *)	1-dim 25G **)
CL	β_{eff}	0.535 8 %	0.535 4 %
	ℓ_p	1.866×10^{-7} S	1.862×10^{-7} S
2B	β_{eff}	0.532 3 %	0.530 6 %
	ℓ_p	1.710×10^{-7} S	1.716×10^{-7} S
4B	β_{eff}	0.527 0 %	0.523 6 %
	ℓ_p	1.515×10^{-7} S	1.578×10^{-7} S

*) 2-dimensional 8-group diffusion calculation by CITATION code.

**) 1-dimensional 25-group diffusion calculation by ARGO code.

Appendix (A8): Stroke

The 600 mm sodium channel in the axial direction in the core was replaced from its end by B_4C simulating control rod 150 mm at a time and the reactivity worth was obtained. Thus obtained stroke curve is shown in Fig. A8. The differences in reactivity worth between, 1/4 and 4/4, 2/4 and 3/4 were not very large. These values were obtained by the critical method.

Appendix (A9): Chemical analysis of B_4C (Denka) and isotopic ratio (PNC)

The chemical analysis (Denka) of the enriched B_4C pellets used in our experiments and isotopic ratio (PNC Tokai Office) measured in Japan are shown in Table A9. These values were used as reference data and not actually used in our experiments.

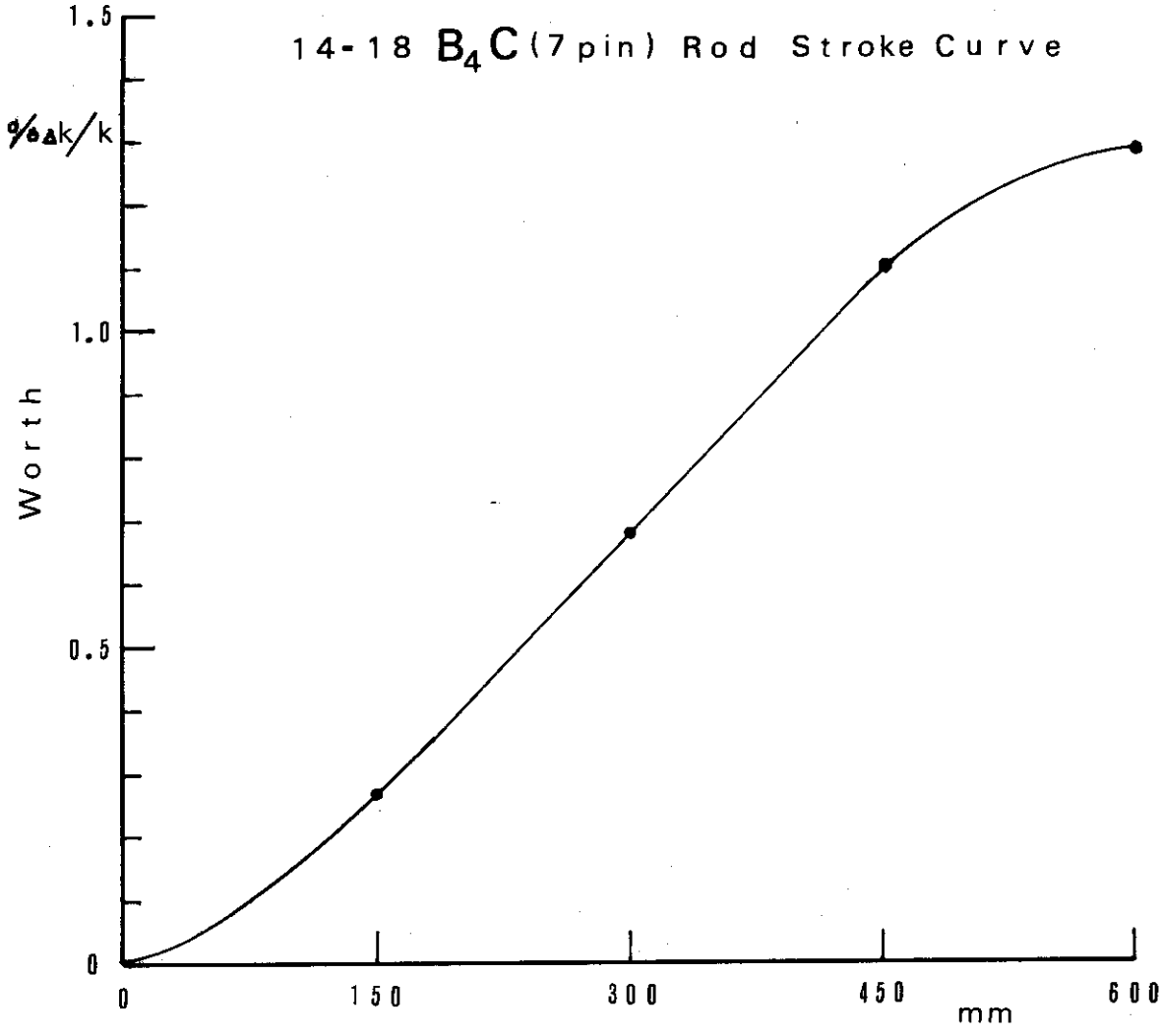

Fig. A8 Rod Position

Table A9 Chemical analysis of B_4C pellet (Denka)

Boron	76.70	%
C	21.80	%
Fe	1000	ppm
Si	>1000	ppm
Al, Ca	100	ppm
Ni	10～100	ppm
Ti, Na	<10	ppm
Mn	1～10	ppm

Boron isotopic analysis by PNC; B^{10} = 90.31±0.20 %